Plasma Treated High Carbon Steel Under Optimized Conditions

By

Atta Ullah

Department of Physics

Quaid-I-Azam University Islamabad, Pakistan

(2023)

Plasma Treated High Carbon Steel Under Optimized Conditions

By

Atta Ullah

Department of Physics
Quaid-I-Azam University Islamabad, Pakistan

(2017-2020)

A DISSERTATION SUBMITTED IN PARTIAL FULFILMENT OF THE REQUIREMENT FOR THE DEGREE OF MASTER OF PHILOSOPHY IN PHYSICS AT THE QUAID-I-AZAM UNIVERSITY, ISLAMABAD 45320, PAKISTAN, JANUARY, 2020.

DECLARATION

I, Atta Ullah s/o Rahmat Khan Registration No. 02181711024, student of M.Phil., in the subject of Physics, session 2017, hereby declare that my dissertation entitled "**Plasma Treated High Carbon Steel Under Optimized Conditions**" is my own work and has not been printed, published or submitted as research work, Dissertation or publication in any form in any university, Research Institution etc. in Pakistan.

Dated: 31th January, 2020

REASEARCH COMPLETION CERTIFICATE

This is to certify that the research work presented in this dissertation entitled **"Plasma Treated High Carbon Steel Under Optimized Conditions"** was conducted by Mr. Atta Ullah, Registration No. 02181711024 under my supervision.

Supervised by:

____

Prof. Dr Muhammad Shafiq

Department of Physics

Quaid-I-Azam University Islamabad.

Submitted Through:

____

Prof. Dr. Kashif Sabeeh

Chairman

Department of Physics

Quaid-I-Azam University Islamabad.

DEDICATED

TO

MY LATE PARENTS

BROTHERS

SISTERS

WIFE

AND

DAUGHTERS

ACKNOWLEDGEMENTS

In the name of Allah, the most Beneficent, the most Merciful. Thanks to the Creator of this universe for showering upon me countless blessings and make me able to complete my M.Phil. dissertation. I would like to thank my Prophet (ﷺ) for remembering me in his prayers.

I am glad to express my deepest gratitude towards Professor Muhammad Shafiq for his kind supervision throughout the whole research. Thanks to the Future doctor, Muhammad Imran Bashir, for directing, assisting, guiding and observing me in the entire work. I would also thank to Higher Education Commission and my family for their financial support. I am more than happy to acknowledge my friends Ahmad Nawaz, Muhammad Abdur Rehman, Muhammad Zeeshan, Mohib Ullah, Irfan Khan and Mudassir Hussain.

Finally, I would like to acknowledge my family members to stay with me through every thick and thin. Special thanks to my brothers, Abd Ullah and Hazrat Ullah for their support. In this occasion, I am glad to remember the kids in our home for entertaining me and relaxing my tiredness. I thank to Wajahat Ullah, Wajeeha Khan, Wajeeh Ullah, Waleejah Khan, Fatima Khan and all other family members from the core of my heart.

Mr. Atta Ullah

Registration No: 02181711024

Contents

Chapter No: 1 INTRODUCTION

Abstract xii

1.1 Plasma 1

1.1.1 Plasma Applications 1

1.1.2 Plasma shielding 2

1.1.2.1 Plasma Sheath 3

1.1.3 Plasma Criteria 4

1.1.3.1 Quasi-Neutrality 5

1.1.3.2 Collective Behavior 6

1.1.4 Plasma Frequency 7

1.2 Classification of Plasma 8

1.2.1 Cold plasma 8

1.2.2 Hot Plasma 9

1.3 Plasma Generation 10

1.3.1 Radio frequency Plasma 10

1.3.1.1 Capacitively Coupled Plasma 10

1.3.1.2 Inductively Coupled Plasma 11

1.4 Material Used in Experiments 12

1.4.1 Steel 12

1.5 Steels Classification by Composition 13

1.5.1 Low Carbon Steel 13

1.5.2 Medium Carbon Steel 13

1.5.3 High Carbon Steel 13

1.6 Grading of Steel 14
1.7 Stainless Steel 16
1.7.1 Chromium & Nickle 16
1.7.2 Molybdenum & Tungsten 17
1.7.3 Nitrogen, Copper and Carbon 17
1.8 Classification of Stainless Steel by Micro-Structure 17
1.8.1 Austenitic Stainless Steel 17
1.8.2 Ferritic Stainless Steel 17
1.8.3 Martensitic stainless steels 18
1.8.4 Duplex stainless steels 18
1.9 Layout of Dissertation 19

Chapter No: 2 DISCHARGES, SPUTTERING AND NITRIDING

2.1 Interactions of Ions with Target-Surface 20
2.2 Sputtering 21
2.2.1 Sputtering Yield 22
2.2.2 Sputtering of Alloys 24
2.3 Discharges in Plasma 26
2.4 DC Glow Discharge 26
2.4.1 Dark Discharge Region 26
2.4.2 Glow Discharge Region 29
2.4.2.1 Regions of Normal Glow Discharge 29
2.4.2.2 Regions of Abnormal Glow Discharge 31
2.4.3 Arc Discharge Region 32
2.5 Pulse DC Glow Discharge 32
2.5.1 Application of Pulse DC Discharges 33
2.6 RF Discharges 33

2.7 Microwave Discharge Plasma....34
2.7.1 Applications of Microwave Plasma....34
2.8 Nitriding....34
2.9 Purpose of Nitriding....35
2.10 Methods of Nitriding....36
2.11 Plasma Nitriding....36

Chapter No: 3

EXPERIMENTAL SETUP AND CHARACTERIZATION TECHNIQUES

3.1 Physical Vapor Deposition (PVD) System....40
3.1.1 Vacuum chamber....41
3.1.2 Pumping & Pneumatic System....42
3.1.3 Turbo Molecular pump....42
3.1.4 Working principle of PVD....43
3.1.5 PVD (Physical Vapor Deposition) Operation Steps.....45
3.2 Cathodic Cage Plasma Nitriding (CCPN) Experimental Set Up....46
3.2.1 CCPN Chamber....47
3.2.2 Cathodic cage....48
3.2.3 Vacuum System....49
3.2.4 Power system....50
3.2.5 Gas Feeding....50
3.3 Characterization Techniques....50
3.3.1 X-rays Diffraction....50
3.3.2 Scanning Electron Microscope (SEM)....52
3.3.3 Micro Hardness Test (MHT)....53
3.3.3.1 Principle of Micro Hardness Test....53
3.3.3.2 Micro Hardness Measurement....55

Chapter No: 4 RESULTS AND DISCUSSION

4.1 Specimens Preparation 57
4.2 Experimental parameters 58
4.2.1 ASPN (Active Screen Plasma Nitriding) Operation Parameters 58
4.2.2 PVD (Physical Vapor Deposition) Operation Parameters. 59
4.3 SEM observations 60
4.3.1 Untreated Specimen 60
4.3.2 ASPN Treated Specimen 61
4.3.3 Single PVD Treated Specimen 61
4.3.4 Duplex Treated Specimen 62
4.4 XRD Spectra 63
4.4.1 XRD Spectrum of Untreated Specimen 63
4.4.2 XRD Spectrum of ASPN Treated Specimen 63
4.4.3 GIXRD Spectrum of Single PVD Treated Specimen 64
4.4.4 GIXRD Spectrum of Duplex Treated Specimen 65
4.5 Hardness observation 65
4.5 Conclusion 67

LIST OF TABLES

Table 1: A comparison among solid, liquid, gas and plasma states of matter....................2

Table 2: Properties of neutral gas versus plasma....................5

Table 3: Major effects and composition limit of different elements in steel....................15

Table 4: Types of Stainless Steel....................18

Table 5: Experimental data of sputtering yield and threshold voltages....................23

Table 6: The chemical composition of Specimens....................58

Table 7: Physical parameters of CCPN operation....................59

Table 8: Physical Parameters of PVD operation....................59

Table 9: Hardness profile of different specimens....................66

LIST OF FIGURES

Figure 1.1: Plasma is separated from the walls by sheath in plasma chamber....................4

Figure 1.2: Different shapes of CCP chambers configured like capacitors in circuit....................10

Figure 1.3: ICP chambers of different shapes....................11

Figure 1.4: Role of carbon in steels (w.r.t to % composition)....................12

Figure 1.5: Classification of steel....................14

Figure 2.1: Possible Ions- Target Interactions....................20

Figure 2.2: A plot of sticking probability vs kinetic energy of ions....................21

Figure 2.3: Angular dependence of sputtering yield....................24

Figure 2.4: I-V Characteristic curve of DC low pressure discharge....................28

Figure 2.5: Pictorial views of glow discharge region....................30

Figure 2.6: Compound and diffusion layers form during nitriding process....................35

Figure 2.7: A typical experimental setup for glow DC plasma nitriding....................38

Figure 2.8: Mechanism of mass transfer in ion nitriding as proposed by Edenhofer....................39

Figure 3.1: The phenomenon of magnetron sputtering 40

Figure 3.2: Chamber of PVD setup 41

Figure 3.3: Inter-connection diagram of pumps, values and PVD chamber. 42

Figure 3.4: Working scheme of turbo molecular pump 43

Figure 3.5: (a) Pictorial diagram of 9 kW turbo pump (Taiyueheng TYFB-1600), (b) Inner Blades view of Turbo Pump 43

Figure 3.6: Motion of electrons and ions in electric and magnetic fields 45

Figure 3.7: Diagram of Cathodic cage plasma Nitriding (CCPN) chamber......................... 47

Figure 3.8: (a) Pictorial diagram of Cathodic cage. (b) Specimen placed inside cage (c) Specimens placed on the ceramic plate. 48

Figure 3.9: Working principle of rotary pump 49

Figure 3.10: Interference pattern of Bragg's law 51

Figure 3.11: Pictorial diagram of X-Ray Diffraction Apparatus... 52

Figure 3.12: Diagram of Scanning electron Microscope (SEM)... 53

Figure 3.13: Pictorial diagram of Vickers hardness tester 54

Figure 3.14: Indentation scheme of Vickers Hardness Tester... 55

Figure 3.15: Schematic Indenter of hardness tester... 56

Figure 4.1(a): Micro-graph of untreated sciencemen has polishing scratches......................... 60

Figure 4.1(b): The SEM micrograph of ASPN treated specimen…………………………… 61

Figure 4.1(c):The SEM micrograph of single PVD treated specimen.................................. 62

Figure 4.1(d): The SEM micrograph of Duplex PVD treated specimen 62

Figure 4.2: X-Ray diffraction analysis of the steel samples.. 64

Figure 4.3: Hardness profile of the High carbon steel.. 67

Abstract

ASPN technique is widely used for the enhancement of the tribological properties of a material's surface in such a way that the properties of bulk material remain unchanged. This technique prevents arcing and edge effects that occur in the other plasma techniques. To enhance the tribological properties further, double layer depositing idea, works. PVD technique has used to deposit a second layer over the substrate of high carbon steel. PVD technique creates good surface outcomes in shorter time and at lower temperatures. Iron Nitride and Titanium Nitride are combined over the high carbon steel to obtain desired results that enhance the tribological properties of the material. Hardness of the ASPN treated specimen increases three times, compared with the untreated specimen. Alloy layer deposition works for the further enhancement of tribological properties.

Chapter No: 1

INTRODUCTION

1.1 Plasma

The word “Plasma” was first introduced by Irving Langmuir in 1927 for “Ionized Gas” in accordance to the “Blood Plasma”. As blood plasma carries red and white blood cells, he thought that ions and electrons were carried by some electrified fluid in the similar fashion. That sort of fluid does not exist, but plasma had got the name from him. Plasma state is one of the four states among solid, liquid and gas states of matter. A brief comparison among these states is shown in table 1. Plasma exists on the earth, in flames, fluorescent lamps, plasma screens, fusion reactors and naturally existing ionosphere (90-400 km above the earth surface) [1]. But it is very common in our universe and makes approximately 99% of our existing universe. Sun, solar wind, nebulae and stars, all of them contain plasma [2-4].

Plasma consists of positive charged ions and negative charged electrons. Neutral species such as atoms, molecules and radicals are also present in this fourth state. The ratio of, charged particles n_i to the neutral particles n_n in a plasma is called the degree of ionization. The ionization degree of plasma can be estimated using the Saha equation given below [5].

$$\frac{n_i}{n_n} \cong 2.4 \times 10^{21} \frac{T^{\frac{3}{2}}}{n_i} e^{-U_i/KT}$$

Where U_i is the ionization energy and T is the temperature of the gas in the above expression. According to Saha equation, nitrogen gas has a degree of ionization $\frac{n_i}{n_n} \approx 10^{-122}$ at room temperature. Plasma may be fully ionized or partially ionized [6].

Scientifically, the word “Plasma” is assigned to the ionized gas and neutral species that carries the properties of quazi-neutrality and collective behavior.

1.1.1 Plasma Applications

Plasma is the future source of energy in the shape of controlled nuclear fusion reaction. Until now, plasma has a wide range of applications, for example in the fabrication of electronic devices and

semiconductors, plasma etching, nuclear fusion, laser plasma, propulsion in space, photo-lithography, plasma processing, radio wave communication through ionosphere, space plasma, hypersonic flight, coating, thin films and magneto-hydrodynamics (MHD) which helps exploring astrophysics [2, 4, 5].

Table 1: A comparison among solid, liquid, gas and plasma states of matter [7]

Solid	Liquid	Gas	Plasma
Ice H_2O	Water H_2O	Steam/Clouds H_2O	Ionized Gas $H_2 \rightarrow 2H^+ + 2e^+$
Cold $T < 0℃$	Warm $0℃ < T < 100℃$	Hot $T > 100℃$	Hotter $T > 10000℃$
Molecules fixed in lattice	Molecules free to move	Molecules free to move, large spacing	Ions and electrons move independent, large spacing.

1.1.2 Plasma shielding

The Debye length λ_D is a parameter of great importance in plasma. It is the radial distance around a charge, beyond which we don't feel the effect of charge, if immersed in plasma. If a surface having charge is immersed in plasma, the corresponding charge species (ions or electrons) will make a cloud around it. Electric field outside the cloud, in a plasma bulk becomes zero. That is, the immersed charge is completely shielded or screened by the surrounded cloud. This phenomenon is named as Debye shielding. Quasi neutrality is also related to Debye shielding [6]. The shield thickness is called Debye length and the cloud is called sheath. λ_D is expressed by the formula (S.I units), given in the following [8]. .

$$\lambda_D = \sqrt{\frac{\varepsilon_0 k_B T_e}{ne^2}}$$

Here ε_0 is permittivity of medium and T_e is the temperature of electrons and n is the density of electrons. The volume of Debye sphere is given by [5]:

$$V_D = \frac{4\pi}{3} {\lambda_D}^3$$

Potential $V(r)$ around positive ions, partially screened by electrons in the Debye sphere, at a radial distance r, is given by [9].

$$V(r) = \frac{1}{4\pi\epsilon_0} \frac{q}{r} \, e^{-\frac{r}{\lambda_D}}$$

It is an exponentially decaying potential and fade down very quickly with increasing r. The systems dimension L must be large enough to vanish the effect of this potential at the plasma bulk, outside the Debye sphere. Which is the origin of the plasma criterion ($L >> \lambda_D$).

The radial distribution of electrons around ions in a Debye sphere is given by [4]:

$$n_e(r) = n_i \, e^{-\frac{qV(r)}{k_B T}}$$

Where T denotes temperature and k_B is Boltzmann's constant.

1.1.2.1 Plasma Sheath

Plasma in a chamber is separated from the walls of the chamber and other surfaces by a thin layer of positive space charges, called plasma sheath. The width of the sheath is less than a centimeter. Plasma sheaths are formed due to the difference between the mobility of electrons and positive ions. Electrons have thermal velocity 600 times greater than ions, therefore they reach the wall earlier and recombine there, leave behind a positively charged plasma [10]. Thus, plasma becomes at positive potential with respect to the wall. The Debye shielding prevents the potential from the distribution over the whole plasma and confines it to a layer as shown in the Figure 1.1.

The width of the layer is constant in DC discharge while in radio frequency discharges, contraction and expansion of the layer occur in an RF cycle. The sheath acts as potential barrier for the electrons and reflects further electron in such a way that it adjusts the number of electrons. Thus

an equal number of electrons and ions reaches per second to the wall and steady state is reached [6].

Sheaths convert electrical energy of the power supply into the kinetic energy of the ions reaching the surface. Electric field in the sheath accelerate ions in a direction perpendicular to the surface. The bombardment energy of ions on the surface is controllable and can be raised up to several thousands time to the binding energy of molecules in solids. This non-thermal plasma process is very useful in surface activation of polymers and ion implantation on semiconductors [10].

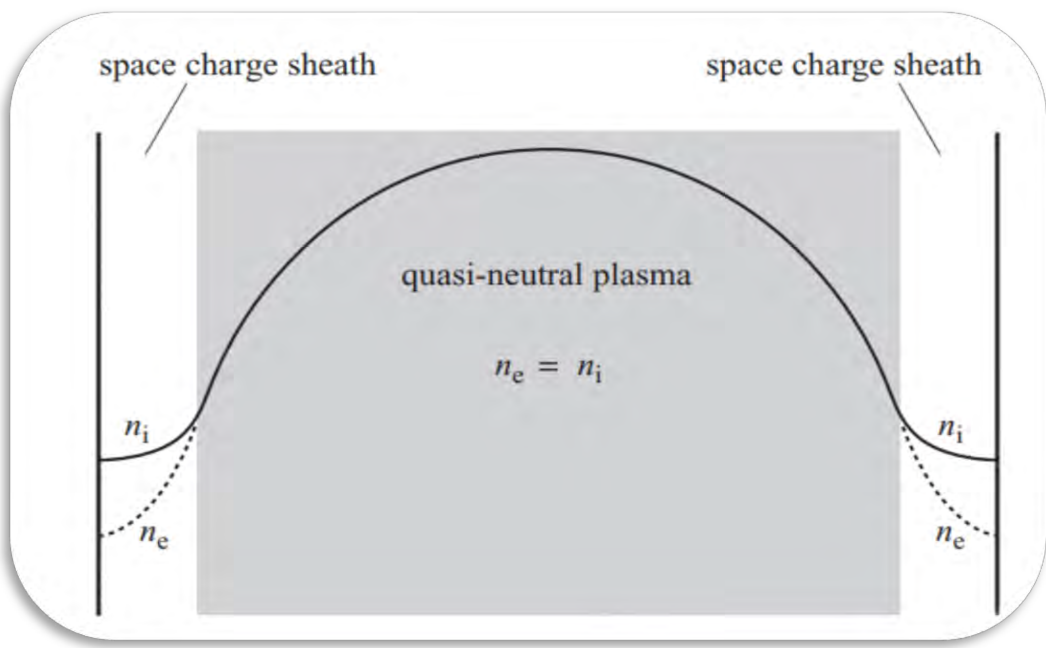

Figure 1.1: Plasma is separated from the walls by sheath in plasma chamber [10]

1.1.3 Plasma Criteria

Although, the fourth state of matter is a kind of ionized gas but it differs enormously from neutral gas. These differences between plasma and neutral gas are illustrated in the table 2. Furthermore, there are certain characteristics that must be obeyed by an ionized gas to be termed as plasma, are given below.

1.1.3.1 Quasi-Neutrality

The density of ions (n_i) is approximately same as the density of electrons (n_e) in a plasma. This characteristic of plasma is called quasi-neutrality. That is;

$$n_i \cong n_e \qquad \text{for singly ionized ions}$$

$$Z_i n_i \cong n_e \qquad \text{for multiply ionized ions}$$

Here, Z_i is the averaged ionized state. The above condition says that the effect of positive charges is equalized by the negative charges' electrons. Thus, plasma as a whole behaves as neutral, but not neutral enough that all the important electromagnetic forces vanish to zero.

Table 2: Properties of neutral gas versus plasma [7]

Property	Gas	Plasma
Electrical Conductivity	Very Low: Air is an excellent insulators.	Usually Very High: For many purposes, the conductivity of plasma may be treated as infinite.
Independently Acting Species	One: all gas particles behave in a similar way, influenced by gravity and by collections like one another.	Two or Three: Electrons, ions, protons, and neutrons can be distinguished by the sign and value of so their charge so that they behave independently in many circumstances.
Velocity Distribution	Maxwellian: Collisions usually lead to a Maxwellian velocity distribution of all gas particles.	Often Non Maxwellian: Collisional interactions are often weak in hot plasmas and external forcing can drive the plasma far from local equilibrium lead to a significant population of unusually fast particles.
Interactions	Binary: Two-particle collisions are the rule, three-body collisions extremely rare.	Collective: Waves, or organized motion of plasma, are very important because the particles can interact at long ranges through the electric and magnetic forces.

1.1.3.2 Collective Behavior

Unlike solid crystals, Plasma consists of unbound particles which are free to move. But plasma particles/species are coupled to each other through electrostatic forces, because both species have charges. A small perturbation anywhere in the plasma bulk, can be felt everywhere due to electrostatic forces. This phenomenon is analogues to a pond-pebble system. When a pebble drops into a pond, disturbs the water in the pond. Furthermore, the disturbance propagates through water waves up to some extent. In this way, water in the pond disturbs collectively, not a small point alone. Similar phenomenon occurs in plasmas, when a charge is brought near the plasma, it effects the whole plasma due to electrostatic interaction. The motion of one species, results the movement of another species. This behavior of plasma is called collective behavior. Unlike neutral gas particles, which interact each other through the collision phenomenon and their parameters are estimated simply by two body collision formulism.

The reason behind the collective behavior is both the electric and magnetic forces. The motion of charge particles produce current which produce magnetic field. When particles move, they get effected by other particles fields. Thus, the elements of plasma effect each other, even at long distances, gives the plasma the characterization of collective-behavior.

Except quasi-neutrality and collective behavior, other characteristics for "ionized gas" to be plasma are [6]:

- The dimension of the plasma must be very large as compare with the Debye length. i.e.

$$\lambda_D << L$$

Where λ_D denotes the Debye length and L denotes the plasma dimension. The size of the chamber requires to be large enough to enclose many Debye spheres inside. This condition ensures quasi-neutrality.

- The total number of shielding charges in the Debye sphere must be large. i.e.

$$N_D >>> 1$$

N_D represents the total number of electrons in the Debye sphere. The above criterion can also be written as:

$$\frac{4\pi{\lambda_D}^3}{3}n_e >>> 1$$

Where $\frac{4\pi{\lambda_D}^3}{3}$ is the volume of the Debye sphere and n_e is the density of electrons.

- Plasma frequency ω_p must be dominant over the collision frequency $\frac{1}{\tau}$.

$$\omega_p\tau > 1$$

ω_p denotes the frequency with which the plasma oscillates, τ is the average time between successive collisions with neutral species. Charges should interact strongly with each other than with the neutral particles in the bulk [4, 6].

1.1.4 Plasma Frequency

In plasma, a uniform positive background is present behind the electrons due to positively charged ions. If the electrons get displaced, an electric field is produced in order to restore the electrons to their previous position for attaining the neutrality of plasma. The electrons overshoot due to inertia and start oscillation around their mean position with a certain frequency called plasma frequency ω_p. The oscillation is so rapid that the ions, due to their heavier mass, are not able to react to the electric field produced by the oscillating electrons, thus ions are considered fixed with respect to their position. Mathematical expression for ω_p is given by the following formula [6].

$$\omega_p = \sqrt{\frac{ne^2}{\varepsilon_0 m_e}}$$

Where n is the number density of electrons and m_e is the mass of electrons. Frequency of plasma is the time constant at which plasma responds to external fluctuation or any change in equilibrium. After applying external fluctuations, plasma tries to acquire a new equilibrium.

Plasma responds to those fields whose frequency are less than plasma frequency and not respond otherwise. If ω is the frequency of applied external field and ω_p is the frequency of plasma, then

$$\omega < \omega_p$$

In this case the dielectric constant of plasma is very high and the energy from the field will be absorbed. However, if the external field frequency ω is greater i.e.

$$\omega > \omega_p$$

Plasma will not respond and will appear transparent to such fields. In this case energy from the field will not be absorbed.

Suppose an alternating voltage ε of frequency ω, having time varying magnitude $\varepsilon = \varepsilon_0 \sin \omega t$ is applied to a plasma between two parallel electrodes. Where ε_0 is the amplitude of the alternating field. According to newton's second law, the equation of motion of electron in the plasma is:

$$m_e \frac{d^2x}{dt^2} = e\varepsilon_0 \sin \omega t$$

The maximum displacement of electron is, therefore:

$$x_0 = \frac{e\varepsilon_0}{m_e \omega^2}$$

The maximum energy gained by the electron is, then:

$$E_0 = \frac{(e\varepsilon_0)^2}{2m_e \omega^2}$$

Frequency of AC generator is $13.56\ MHz$. Angular frequency ω becomes:

$$\omega = 2\pi \times 13.56 \times 10^6 \quad Hz$$

The ionization energy of argon (Ar) is $15.7eV$. Thus, the required amplitude of electric field to provide $15.7eV$ energy to electrons is $11.5\ N/C$.

1.2 Classification of Plasma

1.2.1 Cold plasma

In this type of plasma, temperature of electrons T_e is of the order of 10^5 °K (~10 eV), but the temperature of gas T_g can be as cold as room temperature. This sort of plasma is ionized weakly, called *cold plasma. i.e.*

$$T_g < T_i << T_e$$

Where T_i is the temperature of ions. The above condition clarifies that the thermodynamic equilibrium does not exist in this sort of plasma. The absence of thermodynamic equilibrium in cold plasma is beneficial in commercial uses [2]. Since the electrical energy applied preferentially transferred to the electrons that are heated, meanwhile other particles remain almost at room temperature. These high temperature electrons have the ability to dissociate molecules and convert a gas into reactive species of free radicals and ions. This makes the plasma able to convert electrical energy into chemical or internal energy, which can be utilized in surface modification processes. Cold plasma is a low-pressure plasma and glow discharges are happen in such plasmas. Cold plasma is utilized in many fields, from microelectronic fabrication to the hardening of metallic surfaces.

1.2.2 Hot Plasma

In highly ionized plasma, temperature of electrons T_e is the same as the *temperature of ions* T_i *and* the gas temperature T_{gas} , i.e.,

$$T_e = T_i = T_{gas}$$

Hot plasma is a fully ionized plasma. The above condition says that hot Plasma is locally in thermal equilibrium (LTE). Hot plasma exists if either the temperature of heavy particles is high enough up to 10^6 K (100 eV) *at least,* or pressure of the plasma is high enough up to atmospheric pressure. Under these circumstances hot plasma reaches thermodynamic equilibrium [2].

Higher pressure causes the collision probability between the electrons and ions to increase as well. consequently, as the pressure inside the system increases toward atmospheric pressure, ions and electrons tend to reach the same thermal equilibrium. For instance, thermal plasma is formed in electric arcs, or in plasma jets working at pressures of about 1 atm,.

High temperature plasma is suitable for growth of coatings using plasma spraying processes. It is also used in metallurgy to reduce and smelt ores in the extraction of metals.

Another kind of hot Plasma is CTE (complete thermal equilibrium) plasma. In a CTE plasma, all temperatures are same. CTE plasmas occur in celestial objects (stars etc.) or during the fusion or any other strong explosions. They have no practical or every day importance because they are not yet controllable in the existing laboratory conditions [2].

1.3 Plasma Generation

Plasma can be generated by different techniques, same are given below:-

1.3.1 Radio frequency Plasma

Radio frequency (RF) source can also be used for plasma generation and it is preferred for discharges. When the impurities of electrodes cause the problems, then this RF source is used. Radio frequency ranges from 1kHz to 1000 MHz [11]. However, for plasma generation in the lab we are using 13.56 MHz frequency preferably to overcome the noise that may be produced for radio communication [12]. If power source other than 13.56 MHz frequency is used then proper shielding is required. There are two types of RF coupling which are used for discharges. Capacitively and Inductively Coupled RF Plasma.

1.3.1.1 Capacitively Coupled Plasma

In Capacitively coupled plasma, an alternating source of voltage of radio frequency is used to bias

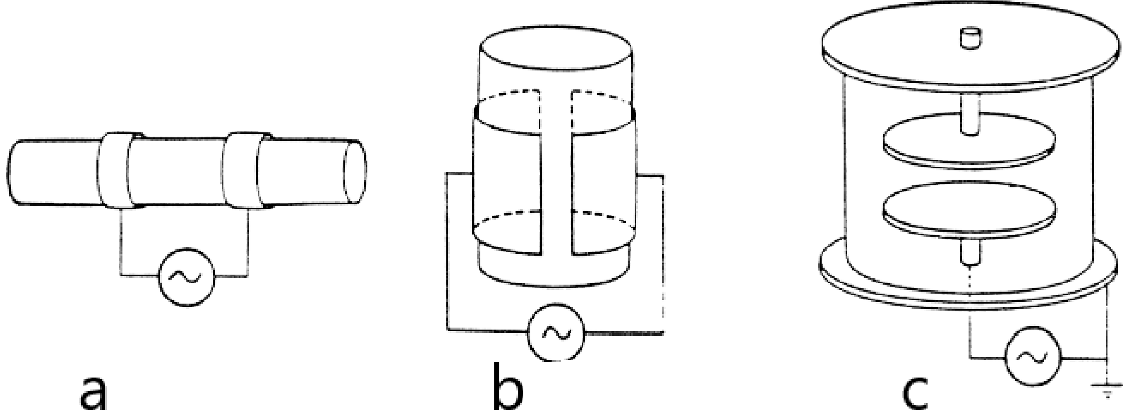

Figure 1.2: Different shapes of CCP chambers configured like capacitors in circuit

one electrode of the plasma chamber while other electrode of the chamber is grounded. The chamber is configured like a capacitor in a circuit, therefore plasma generated in the setup is named as capacitively coupled plasma (CCP). Different CCP chambers are shown in figure 1.2 [8]. CCP technique is applied in industries for dielectric film deposition on different materials that improve their tribological properties [13]. Spectroscopy may be used to analyze the nonconducting properties of materials. According to International communication authorities, the frequency value 13.56 MHz is allotted for the RF generator as a power source. Average value of RF electric field

influences the ions and electrons. The electrons are light as compared to massive ions, so they respond rapidly to the electric field [8].

1.3.1.2 Inductively Coupled Plasma

In 1884, Hittorf developed inductively coupled RF plasma, in which a coil wounded or placed at

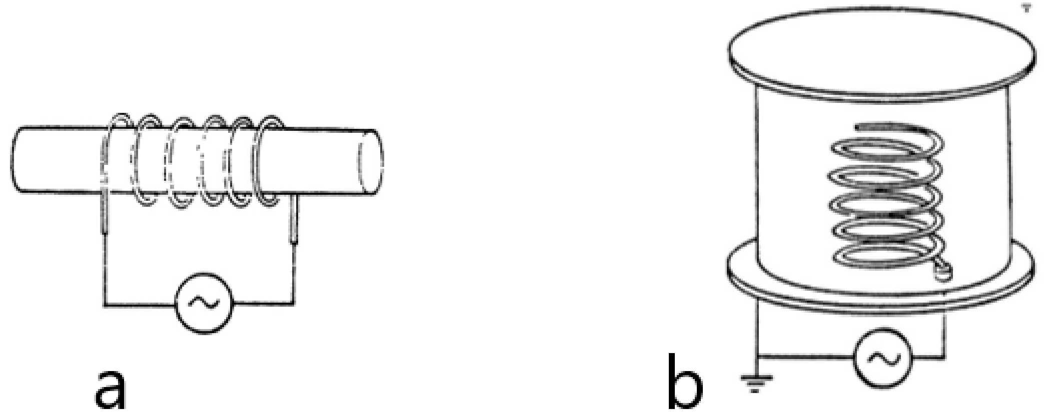

Figure 1.3: ICP chambers of different shapes [8]

the top of the vacuum chamber is biased by RF generator, as shown in figure 1.3. When current passes though the coil, the magnetic field is produced around a current carrying coil. As a consequence of magnetic flux variation inside the plasma region, an electric field is induced. According to Faraday's law;

$$\nabla \times E = -\frac{\partial \mathrm{B}}{\partial \mathrm{t}}$$

Certain voltage is also induced through mutual inductance. Discharge is maintained through an RF electric field of accelerating electrons. Using $\oint E \cdot dl = -d/dt \int B \cdot dS$, The above equation can be written as:

$$V = -\frac{d\phi_m}{dt}$$

Here ϕ_m stands for magnetic flux.

In an inductively coupled system RF plasma will act as secondary coil and upper coil through which current is flowing is called as primary coil. Inductively coupled plasma has a high electron

density, which is about ten times higher as compared to capacitively coupled plasma [14]. There are two modes in inductively coupled plasma.

When the power is low at the initial stage, then the capacitive discharge dominates called E-Mode. As power becomes high it turns into an H-mode (Inductively coupled) and is more luminous due to the high number density of electrons.

1.4 Material Used in Experiments

1.4.1 Steel

Steel is a German language word, means “Standing Firm”. Steel is an alloy of iron with carbon and sometimes other elements including metals and non-metals. Tensile strength, hardness and ductility of steel are dependent on carbon composition percentage present in steel as shown in figure 1.4 [15]. Greater tensile strength and low cost make it a useful material. The density of steel is alloy dependent and found in the range of 7,750 and 8,050 kg/m^3 [16]. Except iron and carbon, other elements are also added to steel in order to obtain desirable characteristics. For example, nickel and manganese gives stability to austinite form and strengthen tensile strength. Melting temperature and hardness can be made higher with the addition of chromium. Vanadium is added for hardness and fatigue purposes.

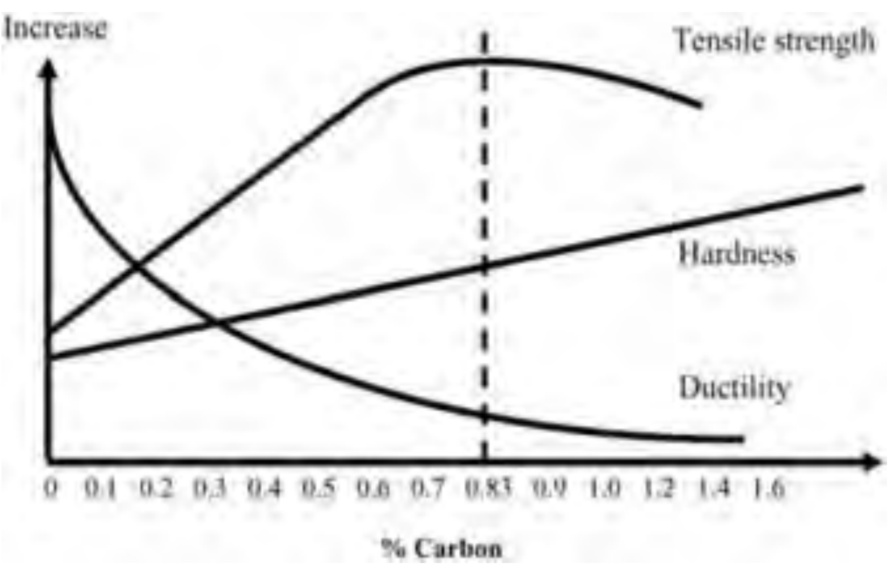

Figure 1.4: Role of carbon in steels (w.r.t to % composition) [15]

Steel is used in tools, vehicles and automobiles, ships and machinery, building and infrastructure, appliances and weapons. Pure iron is a bit resistive to other iron atoms and atoms slide on one another, that's why pure iron is more ductile. The crystal form of Iron depends upon the temperature and can be found in BCC and FCC forms. Alpha ($\alpha - Fe, Ferrite$), gamma ($\gamma - Fe, Austinite$) and Delta($\delta - Fe$) are the iron allotropes having BCC, FCC and BCC crystal structures respectively. Different allotropes of iron have different crystal structures and carbon solubility. $\gamma - Fe$ is the most carbon absorbent which dissolves 2.04 weight percent of carbon at 1419 °K. $\alpha - Fe$ is a poor absorbent of carbon and dissolves only 0.021 weight percent of carbon at 723 °K. $\delta - Fe$ can dissolve up to 0.08 weight percent of carbon at 1748 °K. The addition of carbon in iron made it hard because carbon fits at the interstitial locations in the lattice and reduces ductility of iron. There are different steels corresponds to the different allotropes of iron [17, 18].

1.5 Steels Classification by Composition

Carbon steel has carbon as a major alloying element. Carbon steel is further classified into high carbon, medium, high and ultra-high carbon steels. Carbon steels are the frequently used group of steel [15, 19].

1.5.1 Low Carbon Steel

Steels which contain low carbon contents (0.04 to 0.30 weight percent) are categorized as low carbon steel. They are moldable and can found in almost any shape from sheets to beams. It is used in wire products and vehicles bodies [19].

1.5.2 Medium Carbon Steel

Medium carbon steels contain 0.30 to 0.60 weight percent of carbon and 0.60 to 1.65 weight percent manganese. It is harder and stronger steel but its welding and cutting is difficult. Medium carbon steel re use in gears, axle, cranks, shafts and rails [19].

1.5.3 High Carbon Steel

High carbon steel contains 0.6 to 2 weight percent of carbon [20]. Manganese are present in 0.30 to 0.90 weight percent. It is the hardest and wear resistive steel and used for cutting, drilling and metal pressing [19].

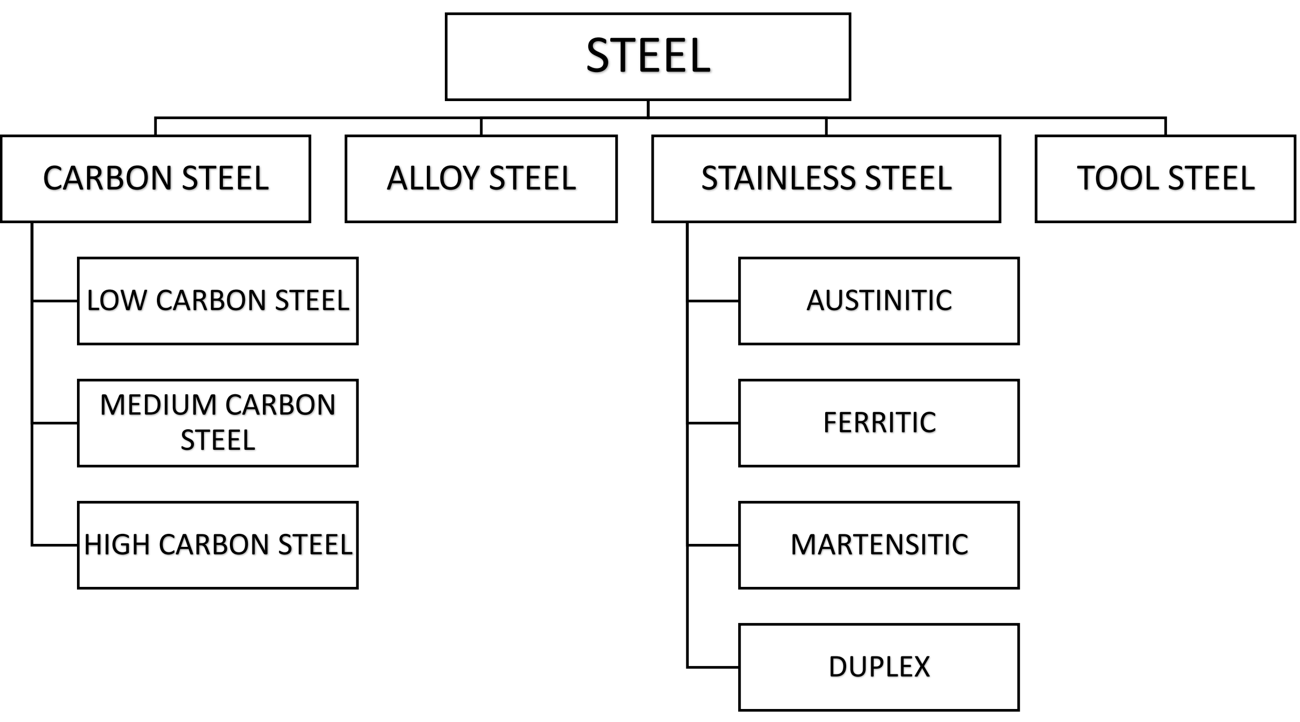

Figure 1.5: Classification of steel [19]

1.6 Grading of Steel

American iron and steel institute (AISI) and society of automotive engineering (SAE) have introduced the grading system of steels based on the alloy composition in a steel. According to the grading system, every steel type is represented by a number, contains four digits. Each digit has its own meaning. 1st digit of steel grades has the following representation [19].

1, Represents carbon (C)steels.

2, Represents the nickel (Ni) alloy steels.

3, Represents nickel-chromium $(\mathrm{Ni-Cr})$ steels.

4, Represents molybdenum (Mo) steels.

Table 3: Major effects and composition limit of different elements in steel [21]

ELEMENT		TYPICAL RANGES IN ALLOY STEELS (%)	PRINCIPAL EFFECTS
Al	Aluminum	< 2	Aids Nitriding, restricts grain froth, removes oxygen in steel melting
S	Sulphur	< 0.005	Add machinability, reduces weldability and ductility
Cr	Chromium	0.3 to 0.4	Increases hardenability, resistance to corrosion & high-temperature strength
Ni	Nickel	0.3 to 5	Promotes an austenitic structure, increases hardenability and toughness
Cu	Copper	0.2 to 0.5	Promotes tenacious oxide film to aid atmospheric corrosion resistance
Mn	Manganese	0.3 to 2	Increases hardenability, promotes an austenitic structure
Si	Silicon	0.2 to 2.5	Removes oxygen in steel making, increases hardenability and toughness
Mo	Molybdenum	0.1 to 0.5	Promote grain refinement, increases hardenability & high-temperature strength
V	Vanadium	0.1 to 0.3	Promotes grain refinement, increases hardenability.

5, Represents chromium (Cr)steels.

6, Represents chromium-vanadium $(Cr - V)$ steels.

7, Represents tungsten-chromium $(W - Cr)$ steels.

8, Represents nickel-chromium-molybdenum $(Ni - Cr - Mo)$ steels.

9, Represents silicon-manganese ($Si - Mn$) steels.

Second digit in the steel grades represents the properties, like concentration of alloys, production methods of steel or any other property. For example;

$10 **$ Represents the carbon steel, having less than or equal to 1 percent manganese ($Mn \leq 1\%$).

$11 **$ Represents resulfurized carbon steels.

$12 **$ Represents resulfurized and rephosphorized carbon steels.

$15 **$ Represents high manganese and non-resulfurized carbon steels.

The final two digits (shown as $**$) represent the concentration of carbon in a steel.

Example 1: 5130 represents chromium steel having 1 percent chromium and 0.30 percent carbon.

Example 2: 1045 represents carbon steel having less than or equal to 1 percent manganese and approximately 0.45 percent carbon [19].

1.7 Stainless Steel

Stainless steel is an in-oxidizable and the most corrosion resistive steel. A steel which contains a minimum 10.5 weight percent of chromium (Cr) and a maximum 1.2 weight percent of carbon (C) is Stainless. Other alloying elements are Nickel (Ni), Molybdenum (Mo), Tungsten (W), Nitrogen (N), Copper (Cu), Titanium (Ti), Niobium (Nb), Zirconium (Zr), Sulphur (S), Cerium (Ce), Manganese (Mn) and silicon (Si). Every alloying element has its benefit which make the stainless steel more useful. The grade number of stainless steel consists of 3 digits, See Table 4 [22].

1.7.1 Chromium & Nickle

Chromium, the most important content in stainlessness, makes the steel corrosion resistive. It forms a thin chromium oxide layer (2-3 nm thickness) which passivate the surface. Adding more chromium makes it more corrosion resistive. Chromium self repairs the surface of steel when damaged, by instant reaction with the oxygen and moisture present in air thus creates a passive oxide layer over the surface. Nickle is an austinite stabilizer and is ideal in acidic environment. It is present 8 to 9 weight percent or more there. Ni prevents general corrosion and allows weldability of steel [23].

1.7.2 Molybdenum & Tungsten

Molybdenum & Tungsten stabilize ferrite in steel. They also improve local and general corrosion resistance which prevent pitting, cracks, crevice and uniform corrosion.

1.7.3 Nitrogen, Copper and Carbon

Nitrogen is added to form austinite micro-structure and strengthen the steel. It is also resistive to local corrosion. Copper is austinite stabilizer and prevents uniform corrosion. Carbon is also an austinite stabilizer and increase hardness. carbon's chromium-carbide is corrosion resistive.

1.8 Classification of Stainless Steel by Micro-Structure

There are four main classes of stainless steel by crystal structure. These are Austenitic, ferritic, martensitic and duplex stainless steel. They are explained briefly in the following.

1.8.1 Austenitic Stainless Steel

The crystal structure of austenitic stainless steel is face centered cubic (FCC), an austenitic microstructure. It is the largest class, about 66% of the total stainless-steel production. Austinite stabilizer alloying element, nickel along with manganese and nitrogen, are added to it in order to sustain its FCC structure. Because it remains in the same FCC structure therefore its strength is independent of temperature. It is weldable, moldable, non-magnetic and ductile class of stainless steel. It has the following two sub-classes [21].

- 200 series
- 300 series

200 series have nickel, chromium and manganese as alloy elements and its strength is 50% more than 300 series due to the nitrogen addition. 300 series have chromium and nickel as alloying elements. AISI 304 has 18% chromium and 8%-10% nickel.

1.8.2 Ferritic Stainless Steel

The crystal structure of ferritic stainless steel is body centered cubic (BCC), a ferritic micro-structure. It contains no nickel or vanish able amount of nickel. The ferrite stabilizer, chromium is present in the 10% to 27% in it. Because it remains in the same BCC structure therefore its strength is independent of temperature. Weldability is poor at more than 2.5 mm thicker sheets. It contains less carbon, corrosion resistive, ferromagnetic and are not heat-treatable.

1.8.3 Martensitic stainless steels

It has a tetragonal body centered microstructure. It contains 12 to 14 weight percent chromium and 0.08 to 0.15 carbon. Martensitic is formed through quenching process from austenitic stainless steel. Quenching is a rapid cooling from high temperatures in water or air. This class of stainless steel is hard and heat treatable. It is ferromagnetic and has low formability. Martensitic steel is not corrosion resistive because of small quantity of chromium. Its welding is poor and produce cracks, must be welded with care. It contains the following four sub-classes.

- Fe-Cr-C grades
- Fe-Cr-Ni-C grades
- Precipitation hardening grades
- Creep-resisting grades [9]

Table 4: Types of Stainless Steel [24]

Types of Stainless Steel		
Types	Major alloy addition	AISI
Ferritic-α	Fe-Cr	$4**$
Austenitic-γ	Fe-Ni-Cr	$2**, 3**$
Martensitic	Fe-Cr-C	$4**, 5**$
Duplex $(\alpha + \gamma)$	Fe-Cr-Ni	
Precipitation hardened	Fe-Cr-Ni	
Super ferrites & Austenitic	Higher Mo & Ni	

1.8.4 Duplex stainless steels

Duplex stainless steel has a mixed micro-structure of austenite and ferrite because it is almost a fifty-fifty combination of austenitic and ferritic stainless steels. It contains a higher chromium and molybdenum contents but lower nickel contents. It is corrosion resistive, more stronger and

ferromagnetic. Its thermal expansion is in between austenitic and ferritic steels. It has the following main sub-classes [25].

- Lean Duplex
- Standard Duplex
- Super Duplex
- Hyper Duplex

1.9 Layout of Dissertation

This dissertation is structured into four chapters. The first chapter introduces plasma, its applications, classifications, and generation, and provides an overview of steels, including stainless steels and their gradings. The second chapter describes the processes of discharging, sputtering, and nitriding. The third chapter outlines the experimental setups for Active Screen Plasma Nitriding (ASPN) and Physical Vapor Deposition (PVD), and discusses the characterization techniques. The fourth and final chapter presents the results from the treated high carbon steel specimens, including findings from the Scanning Electron Microscope (SEM), X-Ray Diffraction (XRD), and Vickers micro hardness tests.

Chapter No: 2

Discharges, Sputtering and Nitriding

2.1 Interactions of Ions with Target-Surface

When energetic ions strike the cathodic surface, several physical and chemical phenomena happen [26-28], as shown in figure 2.1.

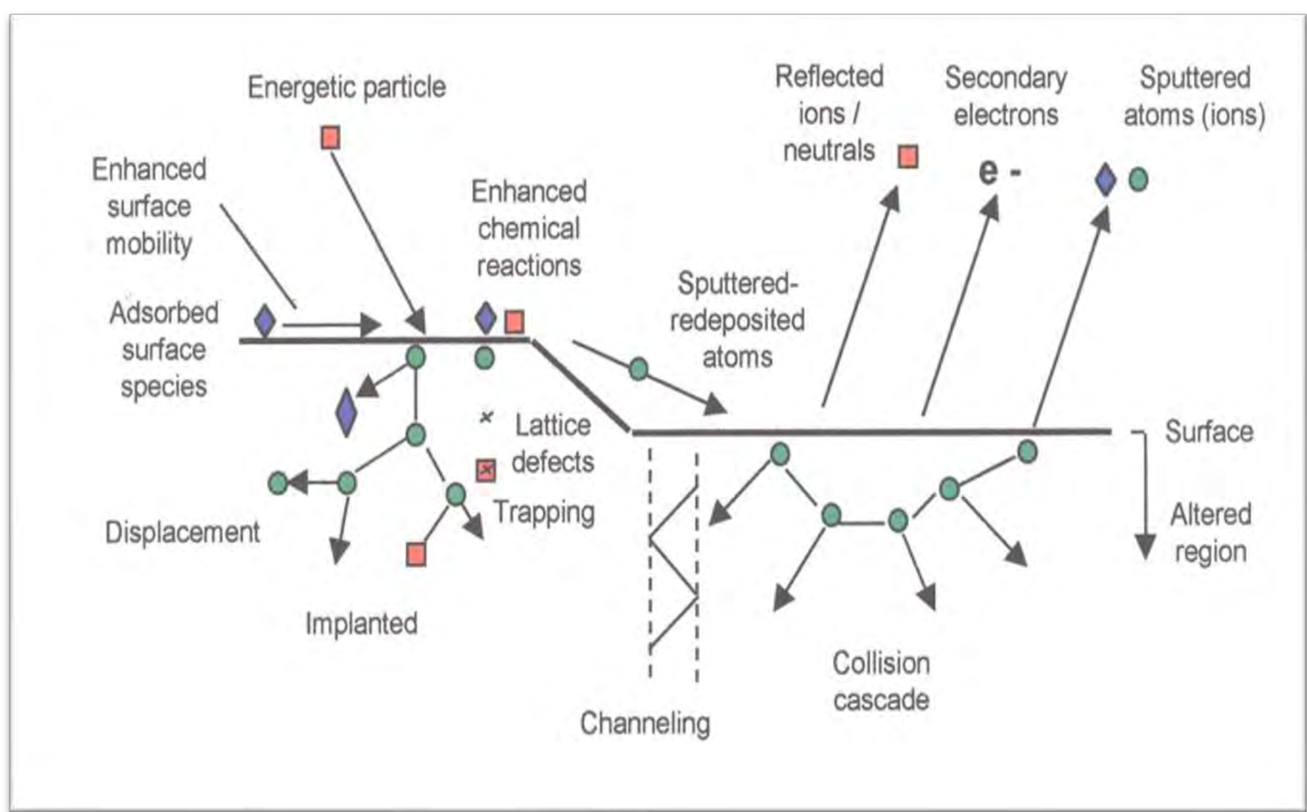

Figure 2.1: Possible Ions- Target Interactions

- *Reflection*: Some of the ions just bounce back of the cathodic surface, after collision.
- *Implantation*: A part of the ions displaces target atoms and penetrate deep into the surface.
- *Absorption:* The ions which have low energy will sit on the target surface and do nothing.
- *Enhanced chemical reactions*: If a gas other than noble gasses has used, it may chemically react with the cathodic material.
- *Channeling*: Some ions may direct into the space between crystal planes called channel, where they experience less resistance and went deeper into the target.

- *Lattice Defects:* Some of the ions can create defects in the lattice of the target material, Amorphization is one them.
- *Sputtering*: Among the ions, some of them remove the atoms of the cathodic material through collision cascade.

2.2 Sputtering

The process of ejecting atoms, ions or molecules from a target material by the bombardment of energetic ions is called sputtering [7]. It is a mechanical process in which sputtering material is deposited on a substrate. Sputtering makes physical vapor deposition more advantageous over chemical and heating processes. The target is set as a cathode, made up of sputtering materials like metals, semiconductors, insulators, oxides, nitrides and fluorides. The target material should be made dense in rectangular, cylindrical or disk shapes. For insulator targets, a conductive baking plate is also used. A cooling mechanism is also used because cathode gets heated when ions strike it.

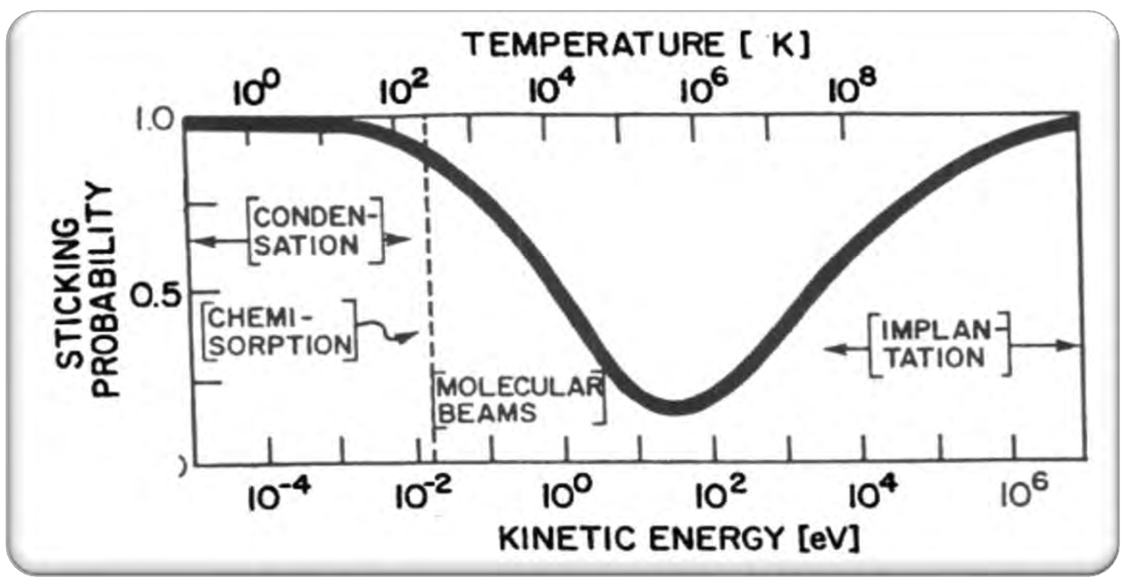

Figure 2.2: A plot of sticking probability vs kinetic energy of ions [29].

Sticking probability is a measurement that how many of the incident ions are possible to adhere or penetrate into a target. During sputtering process, the sticking probability of ions is lowest. Which indicates that sputtering occurs at a certain range ($approximately\, 10 - 100\, eV$) of kinetic energies of ions. In this range of kinetic energy, ions transfer maximum momentum to the atoms

of the target material and eject them out. These ejected atoms are further used for the deposition on a substrate. At lower energies the ions condensate or make a chemical reaction with the target material. At higher energies ions produce the effect of implantation and penetrate deep into the target and reside there. For both higher and lower energies from the sputtering range, the sticking co-efficient is higher [28, 29], as shown in figure 2.2.

2.2.1 Sputtering Yield

Sputtering yield is a measure of the of sputtered atoms to the impinging ions. i.e.

$$Sputtering\ Yield = \frac{number\ of\ sputterd\ atoms}{number\ of\ impinging\ ions}$$

The empirical formula for sputtering yield ($E < 1kev$) is given by [28, 30]:

$$Y = \alpha \frac{Mm}{(M+m)^2} \frac{E}{U}$$

- Here, M is the mass of the target atoms,
  m is mass of the incident ions,
  E is the kinetic energy of ions,
  U is the ionization energy of target atoms,
  α is momentum transfer coefficient.

In the sputtering range Y is directly proportional to E. If the kinetic energy of the incident ions is greater sputtering yield will be greater and vice versa. Sputtering yield depend upon the plasma species as well as the nature of sputtering material. It also requires a certain minimum voltage called threshold voltage. Helium, neon, argon etc. are used as Plasma species in neutral plasma. For different sputtering material sputtering yield is different as shown in the table 5 [28]. Sputtering yield depends upon the following factors.

- *Position of the elements in the periodic table*. Because sputtering yields depends upon the ionization energy of the target material.
- *Crystal structure of the sputtering material*. Also, for the same material, closed packed directions have greeter sputtering yields, because more atoms react with ions in this direction. It results different sputtering yields in different directions.

Table 5: Experimental data of sputtering yield and threshold voltages [28].

Sputtering gas energy (keV) →	He 0.5	Ne 0.5	Ar 0.5	Kr 0.5	Xe 0.5	Ar 1.0	Ar threshold voltage (eV)
Ag	0.20	1.77	3.12	3.27	3.32	3.8	15
Al	0.16	0.73	1.05	0.96	0.82	1.0	13
Au	0.07	1.08	2.40	3.06	3.01	3.6	20
C	0.07	—	0.12	0.13	0.17		
Co	0.13	0.90	1.22	1.08	1.08		25
Cu	0.24	1.80	2.35	2.35	2.05	2.85	17
Fe	0.15	0.88	1.10	1.07	1.0	1.3	20
Ge	0.08	0.68	1.1	1.12	1.04		25
Mo	0.03	0.48	0.80	0.87	0.87	1.13	24
Ni	0.16	1.10	1.45	1.30	1.22	2.2	21
Pt	0.03	0.63	1.40	1.82	1.93		25
Si	0.13	0.48	0.50	0.50	0.42	0.6	
Ta	0.01	0.28	0.57	0.87	0.88		26
Ti	0.07	0.43	0.51	0.48	0.43		20
W	0.01	0.28	0.57	0.91	1.01		33
GaAs		0.10	0.83			1.52	20–25
InP			1.00			1.4	25
GaP			0.87				36
SiC		0.13	0.40				17
InSb			0.50				

- *Amorphization of the surface*. As ions-target interaction can change the crystal structure to amorphous. It means as target gets older, its sputtering yield becomes lower. To restore the surface, one must anneal the target material.
- *Incident angles of the impinging ions*. As explained in the following graph, the ions with incident angles close to 60° have greater sputtering yields while ions yield almost no sputtering incident at an angle of 90°.

Sputtering yields dependent parameters are:

- The energy of the sputtered atoms. Atoms sputter out with different kinetic energies (ranges $2-7eV$).
- The angular distribution of the sputtered atoms. Atoms sputter out with different angles.

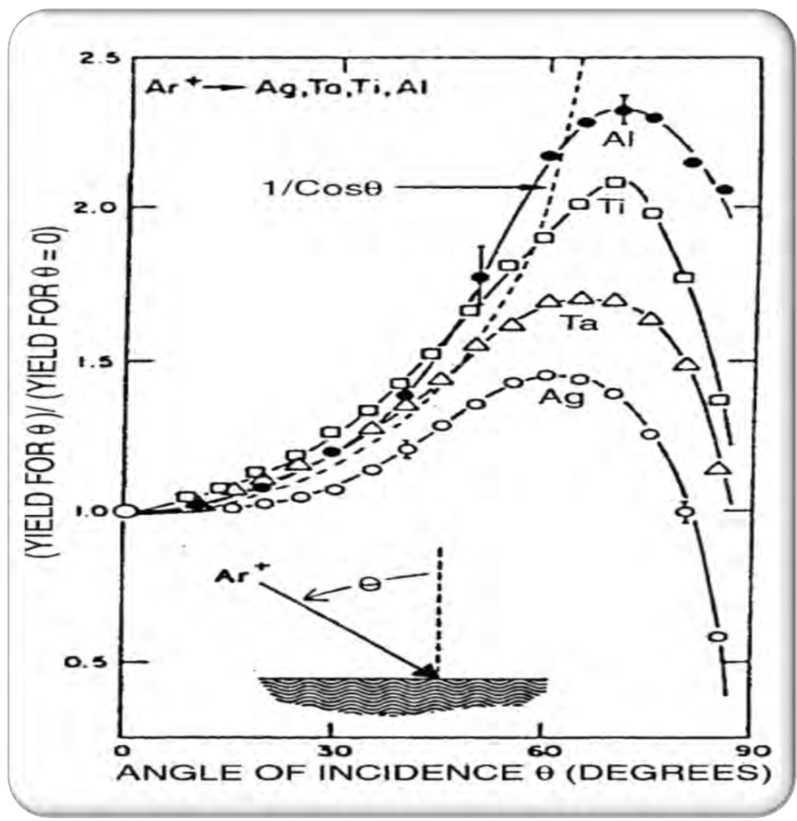

Figure 2.3: Angular dependence of sputtering yield

2.2.2 Sputtering of Alloys

If a target is made up of an alloy, having A and B as alloying elements. Let the N_A and N_B are the number of atoms of elements A and B in the alloy respectively. The total number of atoms present in alloy are N.

$$N = N_A + N_B$$

Let their concentrations are C_A and C_B in the alloy, given in the following.

$$C_A = \frac{N_A}{N}, \qquad C_B = \frac{N_B}{N}$$

Let their sputtering yields are Y_A and Y_B respectively. The sputtered flux of elements is φ_A and φ_B respectively. The sputtered flux is initially given by;

$$\frac{\varphi_A}{\varphi_B} = \frac{C_A Y_A}{C_B Y_B}$$

If n number of ions are incident on target and remove n_A and n_B number of atoms from target, where;

$$n_A = nC_AY_A\,, \quad n_B = nC_BY_B$$

The removal of atoms from the target, modify the concentrations from C_A and C_B to $\acute{C}_A$ and $\acute{C}_B$. Their ratio is now;

$$\frac{\acute{C}_A}{\acute{C}_B} = \frac{C_A(1 - nY_A/N)}{C_B(1 - nY_B/N)}$$

If $Y_A > Y_B$, then the target gets richer in B.

$$\frac{\acute{C}_A}{\acute{C}_B} < \frac{C_A}{C_B}$$

The larger concentration of B atoms, enhances the B flux. i.e.

$$\varphi_B > \varphi_A$$

The flux ratio then becomes:

$$\frac{\acute{\varphi}_A}{\acute{\varphi}_B} = \frac{\acute{C}_AY_A}{\acute{C}_BY_B}$$

or

$$\frac{\acute{\varphi}_A}{\acute{\varphi}_B} = \frac{Y_AC_A(1 - nY_A/N)}{Y_BC_B(1 - nY_B/N)}$$

The continuous change in composition of the target material occur until it reaches a steady state.

$$\frac{\acute{\acute{C}}_A}{\acute{\acute{C}}_B} = \frac{C_AY_A}{C_BY_B}$$

At steady state, the flux of deposition becomes

$$\frac{\acute{\acute{\varphi}}_A}{\acute{\acute{\varphi}}_B} = \frac{C_A}{C_B}$$

This concentration is deposited over a substrate as thin film. Before reaching the steady state, the substrate is blocked by a cover to avoid the deposition of pre-sputtering [28].

2.3 Discharges in Plasma

At industrial level, electric discharges of plasma are mostly used. In a plasma chamber, de-excitation and recombination of atoms give rise the emission of photon in the visible range. Such a luminous discharge is called glow discharges [31]. Glow discharges are used for Tribological properties and surface modification of metals and steels [32, 33], thin films, etching [34] and Sterilization [35]. The DC parallel plate capacitor, plasma reactor and fluorescent lights are applications of DC glow discharge plasma. There are many types of electrical discharges, namely: DC discharges, RF discharges, Microwave discharges, Cyclotron resonance discharges and Electron cyclotron resonance discharges

2.4 DC Glow Discharge

The DC discharges are produced by injecting the gas (argon, helium, nitrogen, etc.) in a chamber at lower pressure (~1 mbar) and supply voltage (~100 V-1 kV) across its conductive electrodes. The general behavior of DC discharge can be understood from current voltage (I-V) characteristic curve described below. Different regions of electrical discharges are produced because current depends upon the applied voltage across the electrodes of the tube. These current, voltage changes in the tube are described in I-V characteristic curve [36] shown in figure 2.4. The I-V characteristic curve consists of the following regions.

- Dark Discharge Region.
- Glow Discharge Region.
- Arc discharge Region.

2.4.1 Dark Discharge Region

It has the following sub-regions [37]:

a) Background ionization.
b) The saturation regime.
c) The Townsend regime.
d) Corona discharges.
e) Electrical breakdown.

(a) Background Ionization

In I-V curve A-B shows the background ionization region. In this region nano ampere current is present in the gas caused by the background radiation or cosmic radiation. These cosmic radiations generate weak ionization due to which a small number of electrons and ions are present.

(b) Saturation Region

The curve B-C indicates the saturation region, which is formed when small external voltage is applied across the electrodes in a gas, but electrons have not sufficient energy for excitation or ionization. That is why current remains constant with the voltage increase.

(c) Townsend Discharge Region

The region beyond point C in dark discharge, is known as Townsend region and current rise exponentially in this region. It is due to the ionization and excitation of gas atoms, when accelerated electrons collide them. Accelerated ions cause the emission of secondary electrons through striking on cathode which are usually known as induced secondary electrons. These induced electrons and ions further collide with neutral gas atoms to produce ionization and excitation. Luminosity is produced in plasma due to electromagnetic radiation emitted during de-excitation.

(d) Corona Region

Corona discharge is represented by curve D-E in I-V diagram. At point E, there are two possibilities due to the large number of electrons in discharge tube. Firstly, if the internal resistance of the power supply is high, large current is not able to flow through a discharge tube. That is why the breakdown of gas does not occur and corona remains in the tube. Its applications are in electrostatic precipitators, ozone formation and photocopying. Secondly, if the internal resistance of the power supply is low, it will cause the breakdown of gas which turns into a glow discharge. In this situation current increases and voltage drops steadily.

(e) Electrical Breakdown Region

The minimum voltage required to obtain the glow discharge is called breakdown voltage, denoted by V_b, and given by Paschen's law as below [38-40].

$$V_b = \frac{Cpd}{ln\left(Bpd/ln\left[1+\left(\frac{1}{\gamma}\right)\right]\right)}$$

Here d is the distance between electrodes and p is the pressure of the gas in newtons per square meter [54]. B and C are experimental constants which depend upon the electron's kinetic temperature and atmosphere of the chamber.

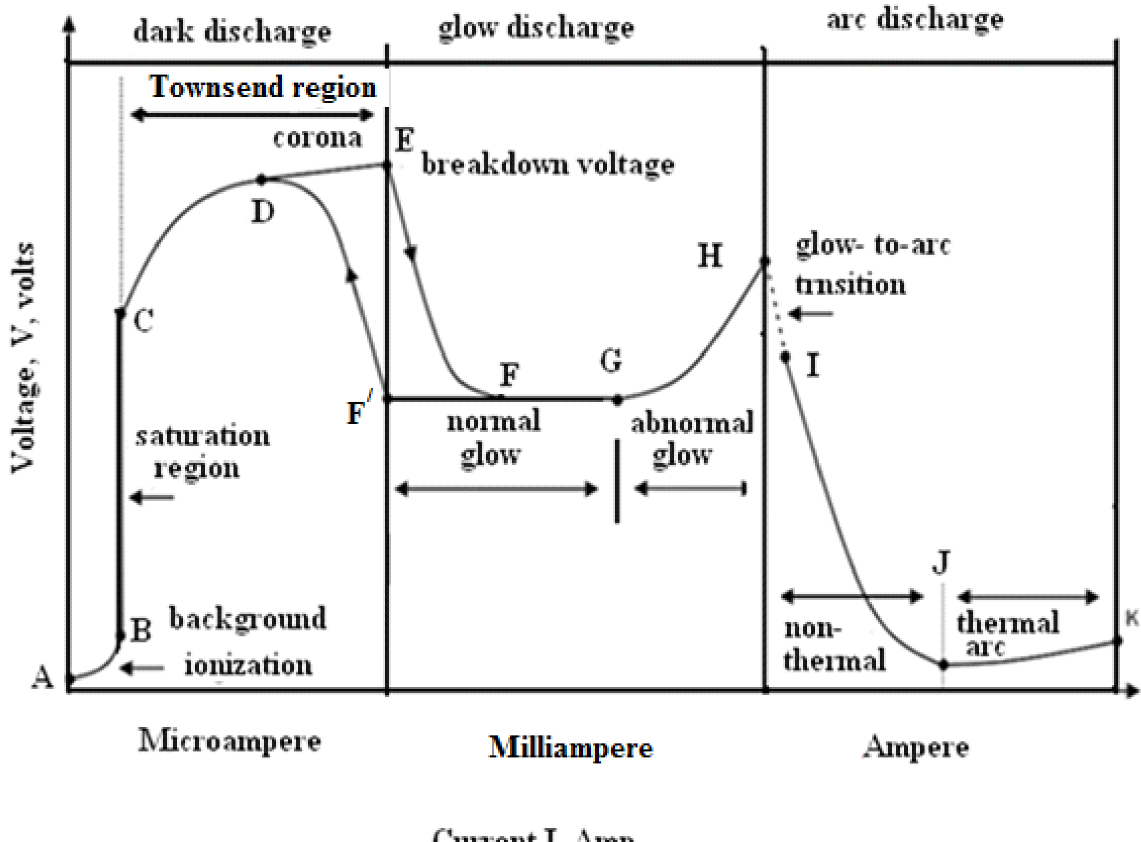

Figure 2.4: *I-V Characteristic curve of DC low pressure discharge.*

γ is the secondary electron emission coefficient given by;

$$\gamma = \frac{No.\ of\ emited\ electrons}{No. of\ incident\ ions\ or\ photons}$$

From this we can see that when the pressure of chamber decreases, Vb also decreases up to some extent initially and then increases. When pressure is fixed, then the breakdown voltage decreases initially with decreasing distance between two electrodes and after certain decreasing, Vb increases. Pressure and mean free path of molecules are inversely related to each other.

While the accelerated electrons ionize the neutral atoms of the gas through external applied voltage, these induced secondary electrons further ionize gas to maintain the glow. But the continuous generation of electrons produces the avalanche breakdown. As the pressure of gas increases collisions increase among the atoms, ions and molecules which decelerate the electrons because the applied electric field cannot accelerate the electrons. The mean free path of electrons for small value of pd increases as compared to electrode distance, by which electrons gain lot of

energy without collisions, that is why high voltage is required for getting more collisions for avalanche breakdown [40].

2.4.2 Glow Discharge Region

It has the following regions

a) The normal glow discharges.
b) The abnormal glow discharges.

The glow discharge region owes its name from the fact that plasma is luminous. This region is shown in the I-V diagram by E-H curve. The glow discharge is due to gas break down, which is due to the occurrence of three processes simultaneously.

- The electric field is sufficient to make collisions of ions with cathode to emit secondary electrons from there.
- These induced secondary electrons further ionize neutral atoms to convert them into ions and electrons.
- Some electrons are lost during diffusion and the collision with walls and by recombining with ions, but the total number of electrons remains constant. The continuous emission of radiation occurs due to recombination of electrons-ions and de-excitation of atoms/molecules/ions which causes the glow to sustain [11].

If the electric field is uniform between two electrodes, then breakdown occurs without preliminary discharge. In case of non-uniform electric field, discharge will start from the region of the highest electric field intensity. This discharge will be at sharp edges and curve points of electrodes due to more effective collisions of ions there. Strong electric field at the edges causes glow discharg. The normal glow discharge region in I-V curve is indicated by E-G. In the normal glow, discharge is produced in the form of a hollow cylinder and the charges starts covering cathodic surface.

2.4.2.1Regions of Normal Glow Discharge

Glow discharge consists of following regions which are based on luminosity [41].

- Aston dark space
- Cathode glow region
- Crooks dark space or cathode dark space
- Negative glow region
- Faraday dark space

- Positive column
- Anode glow region
- Anode dark space region

These eight regions are explained below briefly.

- **Aston Dark Space**

  Just in front of cathode, a region of narrow width but with a strong electric field is present which is called as Aston dark space. In Aston dark space electrons have a small amount of kinetic energy that's why they are unable to excite the gaseous atoms. As there is strong electric field so those electrons are getting more kinetic energy.

- **Cathode Glow Region**

  The next region next to the Aston dark space is cathode glow. This region is merged into Aston dark space depending on the pressure and the nature of the gas used in a classical discharge tube. The gaseous atoms in this region cannot be excited by low kinetic energy electrons. These electrons collide with the positive ions and sputtered atoms which are coming towards the cathode. The radiation, mostly in visible region is emitted due to recombination of ions and electrons.

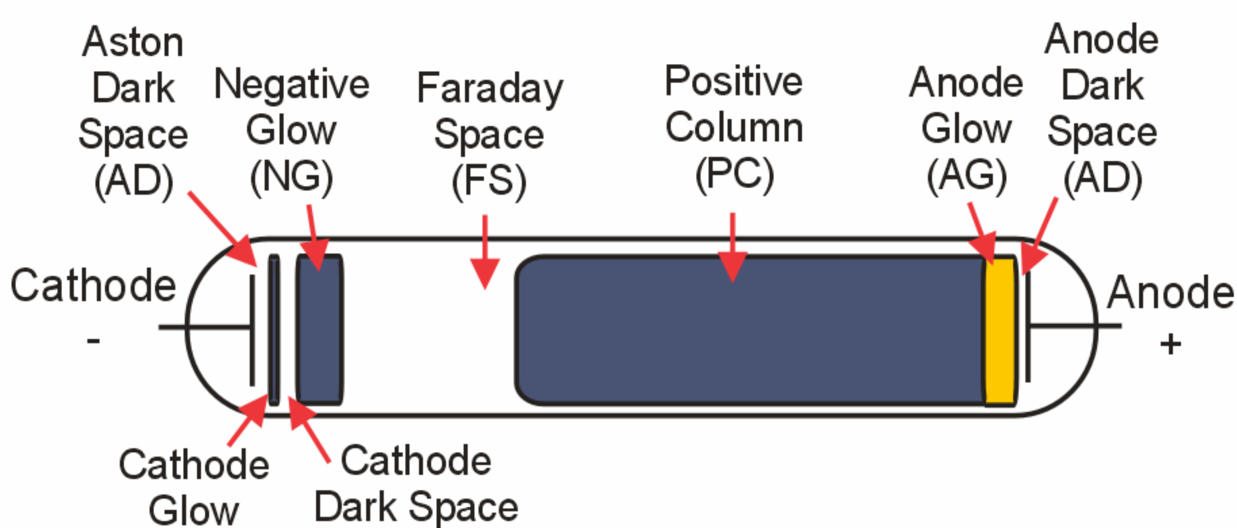

Figure 2.5 : Pictorial views of glow discharge region.

- **Cathode Dark Space / Crooks Dark Space**

  Ions have a high number density due to which there is a more positive space charges relative to the cathode glow. electrons in this region are in the process of gaining energy but still cannot excite or ionize the gaseous atoms.

- **Negative Glow Region**

  Region of negative glow is after the cathode dark space. Here inelastic collisions between electrons and atoms of gas occur. This is the brightest region in glow discharge because electrons have high energy to cause excitation and ionization.

- **Faraday Dark Space**

  As electrons lose their energy after ionization and excitation collisions in the negative glow region and enter the Faraday dark space region. This region is dark because low kinetic energy electrons are unable to excite or ionize. The ions and electrons in this region start to recombine due to which the charge density in this region becomes very small.

- **Positive Column**

  Next to Faraday dark space there is a quasi neutral positive column with weak electric field. The accelerated electrons are not mono-energetic and some high energy electrons can ionize and excite the atoms in this region.

- **Anode Glow Region**

  The brighter region next to the positive column is known as anode glow region. In this region, electrons recombine with ions and as a result radiation are emitted during this process.

- **Anode Dark Region**

  Anode dark space region is present between anode glow and anode. It is formed due to the accumulation of electrons near anode and formation of the sheath of negative space charge. In this region, large number of electrons move towards the anode from the positive column due to the anode pull.

2.4.2.2Regions of Abnormal Glow Discharge

voltage increase slowly in the beginning with increase in the applied current at low pressure. After reaching at point G in I-V curve. Here ions cover the cathode completely and voltage rises. Due to complete covering of cathodic surface, this region is used in plasma processing for uniform treatment [42].

2.4.3 Arc Discharge Region

a) The glow to arc transition.

b) Nonthermal arcs.

c) Thermal arcs.

In arc region, the continuous bombardment of ions makes the cathode heated and starts the emission of electrons thermionically. Current rises due to the excess of free electrons and voltage decreases, causes arc discharge at certain electric field. This value of the electric field is called critical value that remains same for pressure range to be investigated. In electric breakdown region more free electrons due to that current increases and voltage decrease. It is also further sub-divided into non thermal and thermal Arc discharge. Arc discharge has vast applications in everyday life, e.g. plasma cutting, welding and electric discharge machining etc.[43].

2.5 Pulse DC Glow Discharge

If direct current is supplied across electrodes, the cathode heats up due to the continuous bombardment of ions then glow discharge changes into arc discharge. This can damage the cathode if there is no system for proper cooling. On the other hand, when we use alternating voltage across the electrodes, the polarity of cathode and anode changes after every half cycle. We use pulse DC instead of DC with cooling apparatus which is more effective for our system because after each pulse, its discharge reduces for an interval and helps cathode to get cool.

Impact of voltage

There are many industrial applications of pulsed DC . Du Mu and Zheng Yaru established a model for time evolution of DC glow. Glow discharge dynamic behavior is strongly affected by the pulsed voltage according to their model and discharge current also increases by increasing the pulse voltage due to which delay time decreases in discharge.

Impact of distance

As distance among two electrodes decreases, Vb decreases and different glow regions form. If the distance between two electrodes increases, regions like Aston dark space, cathode dark space, cathode glow, negative glow, positive column, Faraday dark space, anode dark space and anode glow etc. form. All other regions vanish by decreasing the distance between electrodes except the negative glow dark space.

2.5.1 Application of Pulse DC Discharges

In material engineering, there are lots of usages of glow discharges through pulsed DC and with the help of pulsed DC we can use high peak values of applied voltages like DC glow discharges. In the DC glow discharges, by increasing the voltage ions energy increase with which they strike on cathode and can damage it. On the other hand, pulse DC gives time to cathode for cooling during its pulsating time. Therefore, in pulse DC glow discharge we can apply high voltage that is direct current flow. It is necessary for adequate ionization, excitation and simultaneous sputtering.

1. With the help of pulse DC plasma discharge we can increase the properties like hardness, corrosion, wear and tear resistance of the surface by nitriding of aluminum steel and titanium etc. [32, 39].
2. Sterilization and decontamination of instruments, especially medical instruments through the pulse DC plasma discharges [35].
3. Diamond like carbon film can be deposited at different materials by using pulse DC [61].
4. An ion source working on pulse DC glow discharge, used in quadruple mass spectrometer.
5. Technique of mass spectroscopy is carried out through pulse DC glow discharge, which is used for conducting and non-conducting material analysis [44].
6. Pulse DC discharge magnetron has been developed. Dielectric films of reproducible formation with good depositing rate and extra high quality are made by using pulse DC discharge magnetron [45].
7. Pulse DC glow discharge plasma is used for doping of semiconductor especially B, BF_1, BF_2, BF_3 can be doped by using pulse DC plasma discharges [46].
8. For the analysis of bulk and depth of different compounds, pulse DC discharges are used for elemental analysis.

2.6 RF Discharges

Radio frequency (RF) source are preferred for discharges, when the impurities of electrodes causes problems. For RF plasma generation in lab, 13.56 MHz frequency is used [11]. There are two types of RF coupling which are used for discharges. Capacitively and Inductively Coupled RF Plasma are discussed in the previous chapter.

2.7 Microwave Discharge Plasma

For producing a typical plasma microwave sources are used, this plasma is named as microwave induced plasma. It requires radiations with frequency range from $300MHz - 10GHz$ to produce plasma. There are different types of microwave plasmas [47]. Some of induced plasmas are the following;

1. Free expanding atmospheric plasma torches
2. Capacitive microwave plasmas (CMPs)
3. Micro strip plasmas (MSPs)
4. Surface wave discharge plasma
5. Resonant cavity plasmas

In these plasmas we must specify pressure limits which is from 0.1pa to some ~2 mbar. The power limits from few to several hundred watts.

2.7.1 Applications of Microwave Plasma

1. For surface improvements and tribological properties modification.
2. Their chemical reactivity is very high that is why we use them for film deposition and etching phenomena at low pressure.
3. At atmospheric pressure, coating is done by microwave discharges [48, 49].

2.8 Nitriding

Nitriding is a process of thermo-chemical diffusion, in which nitrogen atoms can easily be diffused at interstitial sites of the host material (substrate) and make it nitrogeneously enriched. Consequently, material surface become hard, corrosion and wear resistive with the improvement of fatigue life. The solubility limit of nitrogen in materials is usually 2.5 weight percentage. Nitriding occurs when it exceeds the solubility limit. For this purpose, material is heated, usually between 510 and 590 °C, so that nitrogen get stuck with host surface [50, 51]. Nitriding can be used in laboratory as well as in industry for the surface modification of iron alloys such as low carbon and high carbon stain less steels and titanium alloys etc.

Nitrided surfaces mainly consists of two layers. The outer layer called compound layer, mainly composed of two iron nitrides $\acute{\gamma} - Fe_4N$ and $\varepsilon - Fe_{2-3}N$. This layer increases the wear characteristics and impact strength. The inner layer called diffusion layer, mainly composed of

nitrides of alloying elements which improves hardness and surface fatigue life [52]. Fatigue is the weakness caused by repeated variation in stress [53].

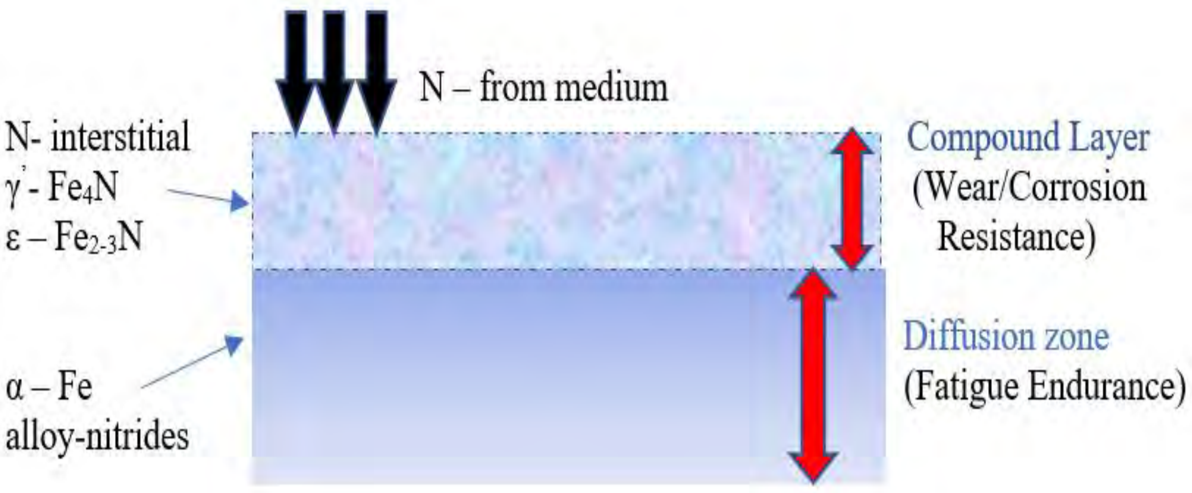

Figure 2.6: Compound and diffusion layers form during nitriding process

2.9 Purpose of Nitriding

Nitriding is done to obtain many purposes. such as, increasing the surface hardness of different soft materials and the reduction of cost. It also used to create materials of lighter weight of the several substances by improving the surface properties such as wear, fatigue, tear and corrosion resistance on small as well as industrial scale. Surface properties of different tools, components and aerospace materials can be achieved according to our needs through surface engineering. Aluminum, molybdenum, steel and theirs alloys are popular because of high strength to weight ratio, easy for engineering, low casting, high electrical and thermal conductivities and preferable for automobile, electronics, aerospace, food processing, conservation etc. uses. However, there is an absence of hardness and corrosion resistance as a result of oxide formation and due to low wear and tear resistances, these materials are smashed when slide over each other. Moreover, the failure in sustaining their shape occurs when stress and strain are applied over them. That is why we require some improvements in their properties for our industrial applications. So, we can use material treatment techniques for achieving our desired qualities. To achieve the material hardness, especially for metals those are strong, resistant to deterioration with low cost of manufacturing. In many industries, nitriding is one of the typical and distinct techniques in its working for improving hardness, morphological properties. Specifically, the nitriding is a valuable surface hardening

technique used for improving tribological properties of metals like molybdenum, aluminum and different steels (SS716, SS304 and SS316). This technique is also used for die-casting tools, forging dies, crankshafts, valves, extruder screws, gears, injectors, aerospace, automobile industry and plastic mold tools etc..

Nitriding technique enhances the performance of materials in the following ways with respect to different parameters.

- The wear resistance increased by nitriding, which helps to oppose the mechanical damage.
- The fatigue resistance increases due to which stress and strain cycle cannot fluctuate the nitrided material due to its stiffness. The geometry of the material is so much sternness that cannot be easily transformed.
- To increase corrosion resistance, we use this awesome technique in which oxides ion removed from the material surface. Nitriding gets rid of corrosion. The interstice filled by nitrogen diffusion, lifting no space for oxides to penetrate [51].

2.10 Methods of Nitriding

Nitriding can be done by using ammonia gas, nitrogenous salt mixture as well as nitrogen gas. In 1913 first time a metallurgical engineer Adolf Machlet working with a US company introduced the nitriding technique through carburizing. The nitriding process started slowly after 1929 and two methods, Gas Nitriding and Salt Bath Nitriding were established [54].

2.11 Plasma Nitriding

The use of glow discharge plasma technique, in order to diffuse Nitrogen ions into a steel or any metallic surface is known as Plasma Nitriding. The purpose of nitriding is to increase corrosion resistance, wear and tear resistance and increase the surface hardness. Plasma Nitriding is widely used in industries because of its low temperature and short-time processing [26].

The plasma nitriding was in full scale production as the General Electric wrote a comprehensive note about the ion nitriding, that there were many problems with these methods. Bernhard Berghaus developed plasma nitriding technique [26] that allowed to nitride all types of materials. This plasma nitriding technique is also called as ion glow discharge, which solved many problems, but he failed to control the discharge. However, after some years Bernhardt Berghaus along with Swiss physicist became able to make plasma nitriding a usable and stabilized technique despite

anything that happened before, yet he neglected to control the release. In 1974, Keller and Edenhofer attempted to clarify the methodology of plasma nitriding and proposed a model [55]. Plasma nitriding has vast favorable circumstances on gas nitriding and salt bath nitriding. In this process, there is less utilization of vigor gas and great control of Nitrided microstructure.

Up to 1980, DC voltage was used for a plasma discharge generation, which has many problems. The main problem with this process was the heating of cathode due to the continuous bombardment of ions during abnormal glow discharge and high value of temperature can damage the apparatus. To overcome this problem, an important progress in the plasma nitriding process was made, that is the development of technique named as pulsed DC plasma nitriding, which tackle the problems of DC plasma nitriding . This process has no negative ecological impacts. However, post discharge nitriding was developed in 1987.

In 1997 Georges developed an active screen plasma nitriding technique that was much better than previous techniques . It has vast applications and can be easily understandable by technicians, engineers, metallurgists and furnace designers now days. This process became more economical and efficient after few modifications [56].

Plasma nitriding is an industrial technique used to make the metallic surfaces hard. In this method, phenomenon of glow discharge is used to diffuse the nitrogen ions into the metallic surfaces in the presence of plasma environment. The life span and tribomechanical properties of soft metallic surfaces can be enhanced via this procedure. In this nitriding, by intense electric field, gas is ionized in the chamber which converts the gas into a plasma state. This ionization of gas causes emission of radiation, which makes the plasma luminous that is why it is called glow discharge. This glow discharge can be seen through the viewing screen. As the glow discharge is established, ions are accelerated through high voltage to strike on the grounded metallic surface. Due to these collisions, the temperature of the metallic surface rises. To raise the plasma temperature, an external heater may also be used. This rise in temperature is necessary for the easy diffusion of nitrogen ions into the sample surfaces. For plasma nitriding, N_2, H_2 and Ar gasses are generally used for processing. Initially argon discharge is used for cleaning impurities from the surface of the specimens. After that N_2 with H_2 is introduced to nitride the sample surface where hydrogen is for removing the oxide layer.

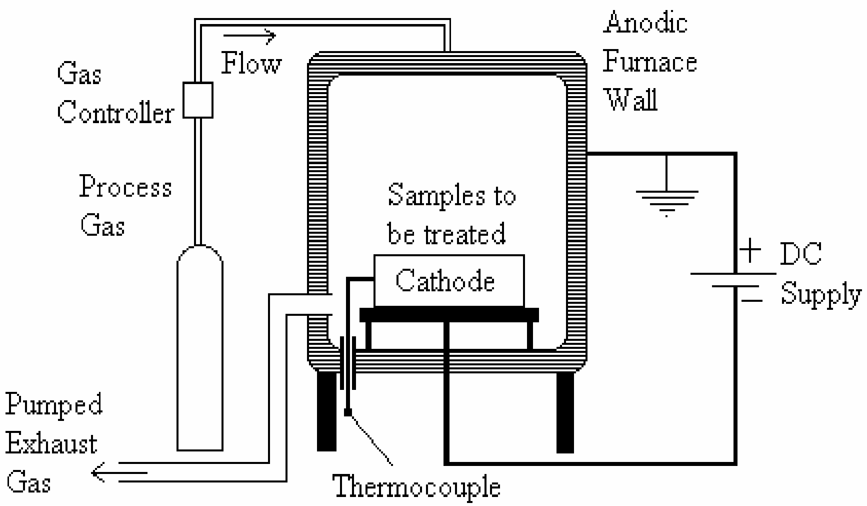

Figure 2.7: A typical experimental setup for glow DC plasma nitriding

Following are some important parameters in this process;

- Treatment time
- Substrate temperature
- Gas pressure in the chamber
- Gas composition.

Besides the applied current density and voltage, some other important parameters also play vital role in plasma nitriding. Till 1965, nitriding mechanism was not clear. In 1973, Hudis was used to nitride the sample by RF discharge. From this he concluded that ions play vital role in nitriding of a sample surface. Tibbit investigated that neutral species and diffusion of atomic nitrogen into a lattice of sample plays a significant role in nitrogen. Kolbel's assumed iron atoms after sputtering from the cathode surface react with the gaseous nitrogen and form a layer of ferrous nitride on the surface of the sample. Due to high temperature, nitrogen atoms from this layer can diffuse into the lattice. The Edenhofer described the principle of mass transfer mechanism, which is based on sputtering and re-deposition. He anticipated that the atoms of Fe are sputtered from the surface due to high cathodic potential and nitrogen ions are used to sputter the specimen surface [52, 57]. The deposition of ferrous nitride occurs on the specimen surface after sputtering. these atoms of Fe recombine with nitrogen atoms. Li *et al.* [55] investigated that direct current plasma nitriding

cannot produce homogeneous temperature, so this is effective only in the case for simple homogeneous loads.

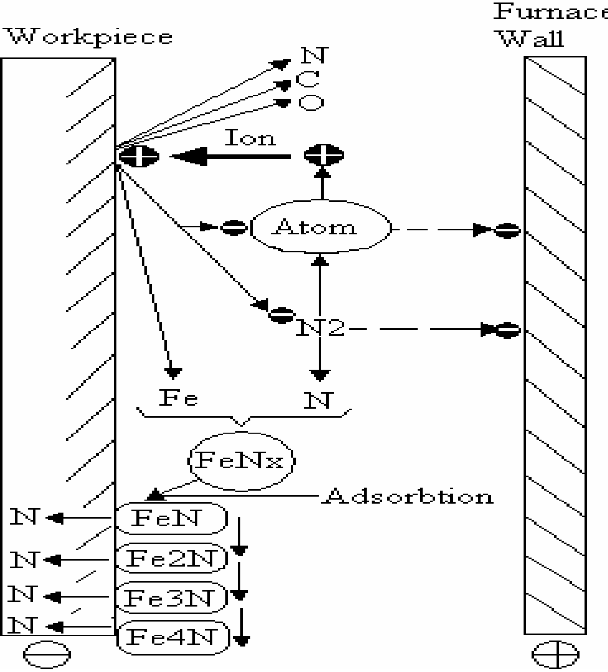

Figure 2.8: Mechanism of mass transfer in ion nitriding as proposed by Edenhofer.

Li et al. [55] concludes that DCPN is only preferable for simple homogeneous load because plasma forms on the load in this case and hence uniform homogenous temperature cannot be obtained.

Advantages:

1. It is easy and short timing treatment process.
2. It improves tribological and tribomechanical properties which include surface hardening fatigue wear and tear resistance by forming a composite layer on the surface material.
3. It controls the Nitrided microstructure.
4. The machine is ready to use after nitriding.

Disadvantages:

1. The apparatus used in this experiment is very expensive.
2. The temperature cannot be controlled efficiently.
3. There is non-uniformity due to arcing problem.

Chapter No: 3

Experimental setup and Characterization Techniques

3.1 Physical Vapor Deposition (PVD) System

The physical vapor deposition (PVD) system consists of SINOARC 306. It has two magnetrons and two arc evaporators [58, 59]. It works on the principle of direct current (DC) magnetron sputtering. In magnetron sputtering, a magnet behind the cathodic target is inserted to enhance the collision probability of electrons with atoms in order to improve sputtering efficiency. In such sputtering, electrons are trapped near the target by a magnetic field such that they are used repeatedly for ionization [60], as shown in figure 3.1.

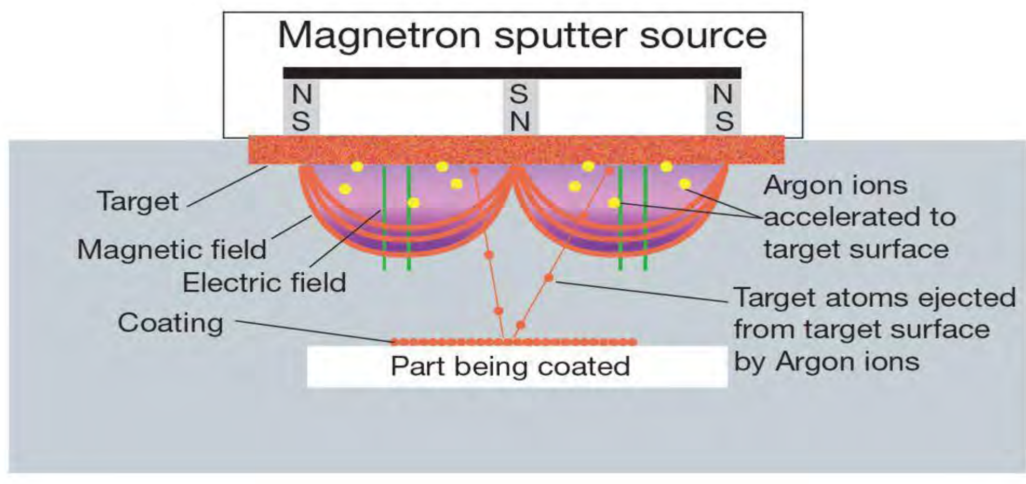

Figure 3.1: The phenomenon of magnetron sputtering [60]

Figure 3.1 shows that magnetic field lines directed from north to south pole of a permanent magnet, fixed behind the target. Electric field is applied perpendicular to the magnetic field. The charged particles move under the influence of both fields. Ions in the plasma hit the target and come out with the ejection of sputtered atoms.

The PVD system (SINOARC 306) has the following major parts.

- Vacuum chamber
- Pneumatic & pumping system

- Gas feeding system
- Heater
- Vacuum measuring system
- Cooling system
- Control system
- Power system

3.1.1 Vacuum chamber

The Physical vapor deposition apparatus has an octagonal prism shape as shown in figure 3.2. The height of the vacuum chamber is 480 mm and side length is 280 mm each [58, 59].

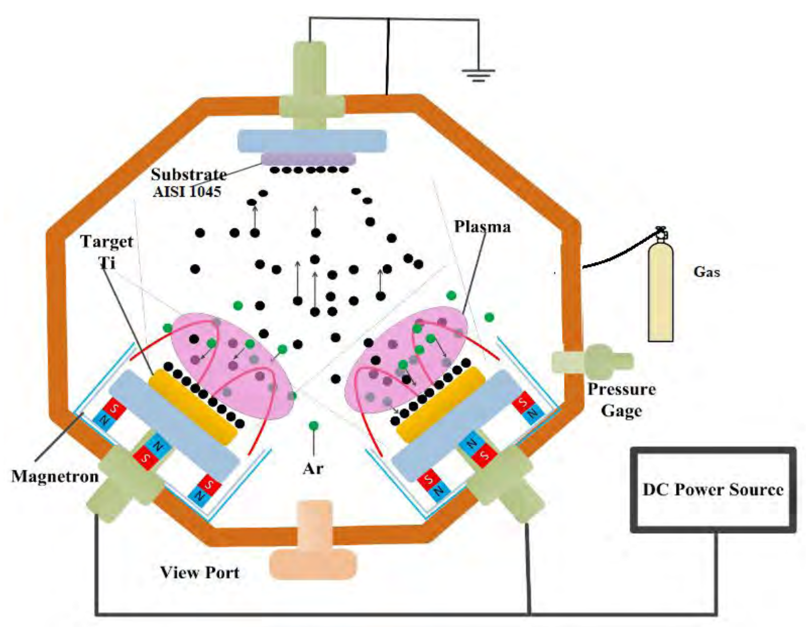

Figure 3.2: Chamber of PVD setup [59]

For chamber evacuation, vacuum system is connected to the chamber. It has a double wall structure, made up of stainless steel. A mesh of water pipes is spread between the walls to insure cooling of the chamber and cathodes through circulating water. Cooling water inlet and outlet are all positioned at the back side of the lower part of the chamber. Mass flow control and heating system is also connected to the chamber through pipes. Two magnetrons and two arc evaporators are installed around the wall along with two viewports. The dimension of magnetrons is such that their radii are 64 mm and thickness 70 mm each. The chamber has a front opening door and a viewport is mounted on the door. Another viewport on the wall is installed opposite to the door.

For loading specimens, a planetary rotating rack is present inside the chamber which can rotate inside the chamber. The specimens are placed at the rack for deposition.

3.1.2 Pumping & Pneumatic System

There are two pumps, backing pump and main pump that evacuate the chamber of PVD. Main pump is 9 kW turbo pump (Taiyueheng TYFB-1600) as shown in figure 3.5 (a & b). It has a pumping speed of 3600 Liters per second. The backing pump is cerlikon leybold vacuum TRIVAC D60C. it makes rough vacuum for the turbo pump. Four pneumatic valves are also used in the system which can be open or close in a specific order to connect or disconnect parts with pumps to be evacuated. Pumps and valves are interconnected and with the chamber by tubes. The connection of pumps and valves with chamber, as displayed on the PVD control screen is shown in the following figure 3.3. P_2 is turbo pump, p_3 is rotary pump. Value V_0 can rotate from 0^0 to 90^0.

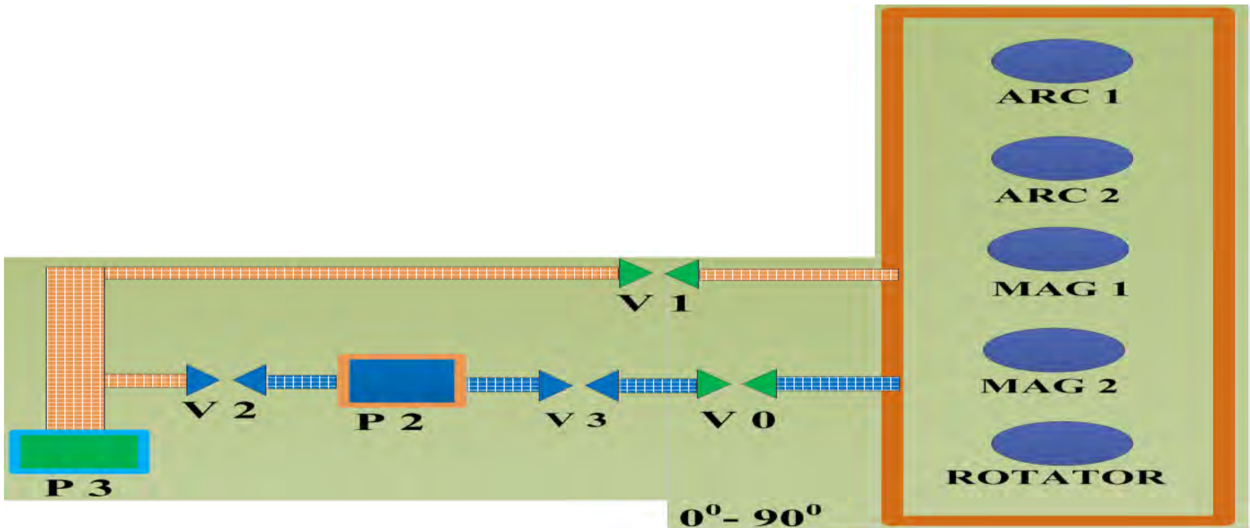

Figure 3.3: Inter-connection diagram of pumps, values and PVD chamber.

3.1.3 Turbo Molecular pump

The structure of Turbo molecular pump is designed in such a way that it gives momentum to the molecules of gas in the chosen direction. For this purpose, optimized spinning angled blades are installed around the shaft that transfer momentum to the air molecules by successive collisions. Blades hit molecules entered through inlet and speed them up in the direction of outlet. The combination of stator and rotator blades compressed the air such that the backing pump gets able to exhaust it from the chamber [61, 62], as shown in figure 3.4. According to the provided specification, Taiyueheng TYFB-1600 has a vacuum range of 10^{-1} to 10^{-6} pascals.

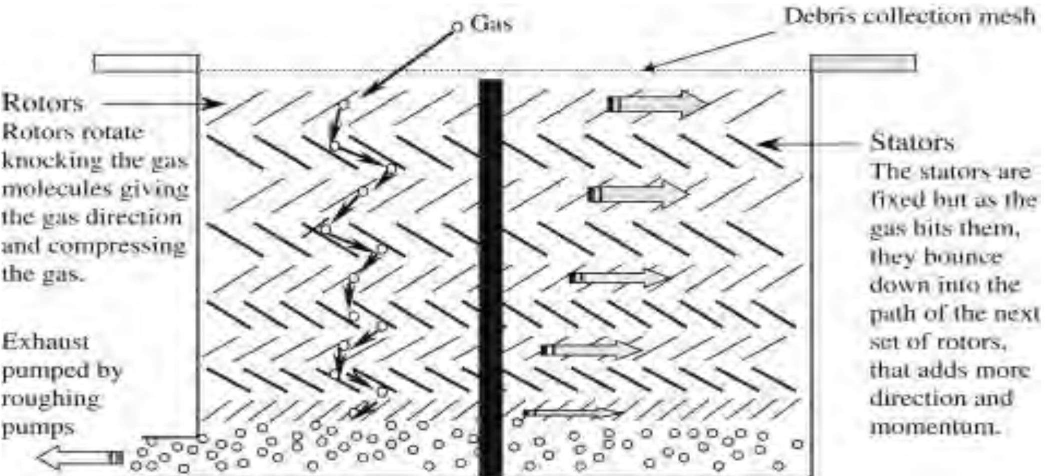

Figure 3.4: Working scheme of turbo molecular pump

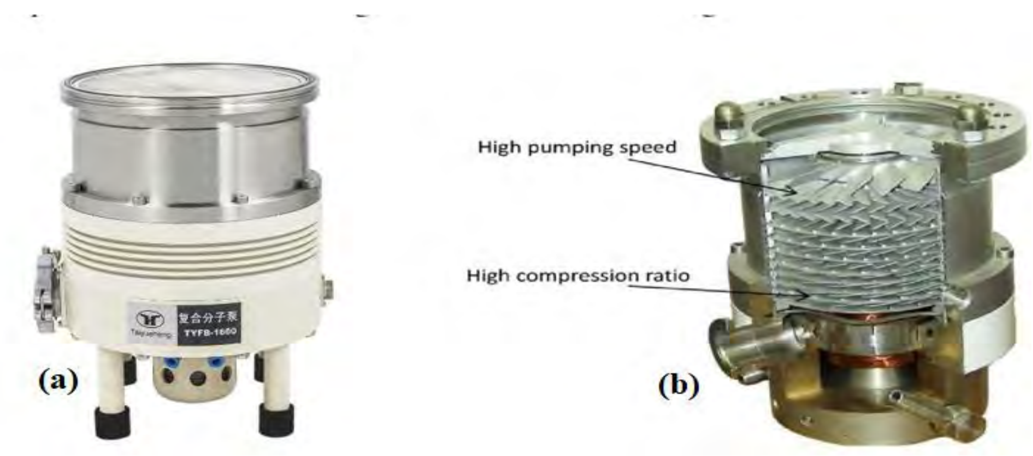

Figure 3.5: (a) Pictorial diagram of 9 kW turbo pump (Taiyueheng TYFB-1600), (b) Inner Blades view of Turbo Pump

3.1.4 Working principle of PVD

The efficiency of sputtering w.r.t energy of incident ions is quite low and about 95% of energy is lost in the form of heat. The sputtered atoms obtain only $3-7ev$ energy from $\sim kev$ impinging ions. In order to increase the efficiency, magnetron sputtering technique is used. In this technique, magnetic field along with electric field is also used for sputtering. In the presence of magnetic field

electrons gyrate in helical paths near the target and get trapped close to the target which ionize atoms repeatedly.

Electrons move under the influence of electric and magnetic fields and experience Lorentz force. If, for simplicity, we choose only one electron, force is given by:

$$\boldsymbol{F} = e\boldsymbol{E} + e\boldsymbol{v} \times \boldsymbol{B}$$

or

$$m\,\frac{\boldsymbol{dv}}{\boldsymbol{dt}} = e(\boldsymbol{E} + \boldsymbol{v} \times \boldsymbol{B})$$

if $\boldsymbol{E}$ lie in the x-z plane and $\boldsymbol{B}$ is assumed to be only in the z-direction,

$$\boldsymbol{E_y} = 0 \quad and\ \boldsymbol{B} = B\hat{z}$$

or in components form,

$$\frac{dv_x}{dt} = \frac{q}{m}E_x \pm \omega_c v_y$$

$$\frac{dv_y}{dt} = 0 \mp \omega_c v_x$$

$$\frac{dv_z}{dt} = \frac{q}{m}E_x$$

v_x and v_y are coupled equations, solving by differentiation we get the following result.

$$v_x = v_\perp e^{i\omega_c t}$$

$$v_y = \pm i v_\perp e^{i\omega_c t} - \frac{E_x}{B}$$

Where $v_\perp$: velocity component perpendicular to magnetic field B.

ω_c: the cyclotron frequency and $\omega_c = \frac{qB}{m}$

The velocities in the above equations are oscillatory velocities (because i is there) around a drift center. The oscillation radius r_L, called Larmor radius, is given by:

$$r_L = \frac{mv}{qB}$$

The above discussion concludes that the motion of electron is helical. A similar motion is also performed by the ion with a bigger radius, as shown in figure 3.6.

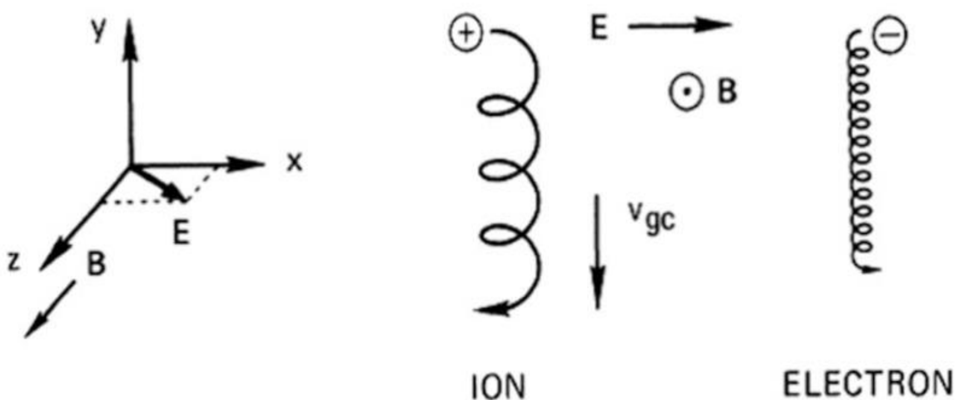

Figure 3.6: Motion of electrons and ions in electric and magnetic fields [6]

The drift of the guided center is given by:

$$\boldsymbol{v}_{gc} = \frac{\boldsymbol{E} \times \boldsymbol{B}}{B^2}$$

The direction of $\boldsymbol{v}_{gc}$is perpendicular to both electric and magnetic fields. Note that, if B and E fields are uniform, the directionality of $\boldsymbol{v}_{gc}$ does not dependent upon charge q, mass m, and velocity v. Ions and electron drift due to the E field in the same direction, but oscillating around their guiding centers in different direction. However, ions move a larger Larmor radius because of heavier mass. Mostly, ions have even lager Larmor radius than the plasmas dimensions [5].

3.1.5 PVD (Physical Vapor Deposition) Operation Steps.

The experimental steps followed during PVD experiment are given in the following.

- Turn on Pneumatic Pump and wait until Pneumatic pressure reaches up to 6 bars.
- power on the system. Pressure display gauge ZJ10 auto ON.
- Press VENT button to get the air in and lose previous vacuum.
- Door opens, when chamber pressure equals atmospheric pressure.
- Load specimens in the chamber.
- Turn ON the rotator and adjust the specimens close to the magnetron.

- ON the chiller along with water pump, compressor 1 and compressor 2.
- ON the rotary vane pump P_3.
- open the valve V_2.
- wait until backing pressure reaches 5 Pascals.
- turn OFF valve V_2.
- turn ON valve V_1. It takes few seconds to get ON (around 5 seconds), after pressing V_1 button. Valve V_1 extends rough pumping towards the chamber.
- ZJ10 florescence auto ON after chamber pressure reaches 7 pascals.
- Wait until chamber pressure reaches 1 Pascal.
- Turn ON the main pump P_2.
- ON the heater. Temperature reaches to the pre-set value. ($T = 150\ °C$).
- ON the high vacuum valve V_3.
- V_0 can rotate from 0° to 90° with respect to V_3. Pressure reaches to the base value 1.2×10^{-2} Pascals.
- Open Argon gas, ON the MFC (Mass flow control) button.
  ($Amount\ of\ argon\ =\ 30\ sccm\ , chamber\ pressure = 7\ pascals$)
- ON DC voltage.
  ($Voltage\ \ V = -10\ volts$)
- Power ON Magnetron (Titanium Cathode)
  ($Power\ \ P = 400\ watts$)
  (Argon removes impurities and sputters cathode. ($time =\ 30\ minutes$))
- Start pure nitrogen gas for reactive sputtering. (Ar/N_2: $19/4$)%
  (Processing time is 40 $minutes$).
- Power off heater.
- Turn off gasses flow.
- Wait until chamber temperature reaches room temperature.
- Turn off the pumps and values (in the reverse order).
- Press VENT. Door opens, collect the coated specimens and place them in a protective case.

3.2 Cathodic Cage Plasma Nitriding (CCPN) Experimental Set Up

Cathodic Cage Plasma Nitriding (CCPN) apparatus has the following major parts.

- CCPN Chamber
- Cathodic cage
- Vacuum System
- Power System
- Heater
- Cooling mechanism
- Gas Feeding System
- Mass Flow Measuring Meters

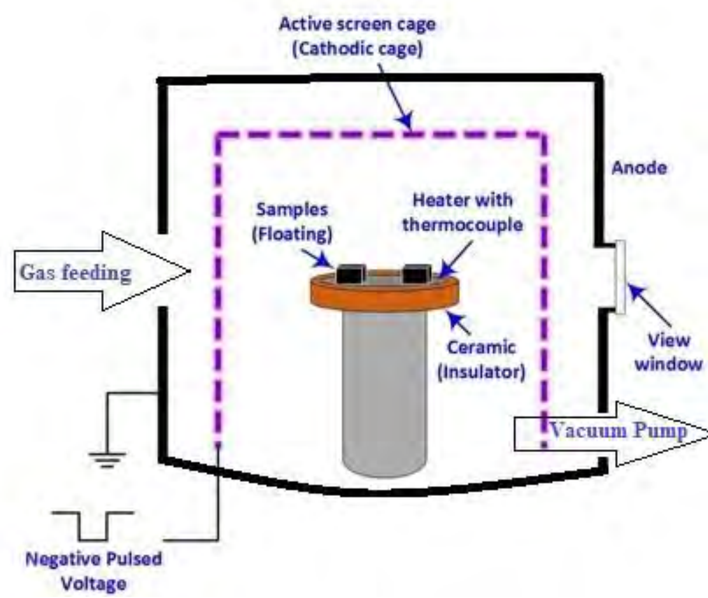

Figure 3.7: Diagram of Cathodic cage plasma Nitriding (CCPN) chamber

3.2.1 CCPN Chamber

The chamber of cathodic cage plasma nitriding experimental setup is made up of stainless steel. It is a locally constructed cylindrical chamber. The diameter of cylinder is 316 mm and height is 335 mm. chamber consists of 8 larger ports (10 cm diameter), one of them is used as a viewing port and has a quartz glass over it. The viewing port is used to sight the glow discharge and for other plasma examine techniques such as OES. Other ports are closed by stainless steel covers. Three out of four smaller ports (25 mm diameter) of the chamber are used for gas feeding and one for pressure gauge attachment [63]. Vacuum pump is attached to one of the four medium sized ports (4 cm diameter). The walls of the chamber are grounded and act as anode. The cage placed inside the chamber is given negative pulsed DC voltage and acts a cathode. A ceramic plate is placed at

the center of the chamber and inside the cage for specimen loading. This ceramic plate isolates the specimens from the anode. An external heater is connected to the bottom of the chamber for rising the temperature of plasma. A thermocouple is also connected with the chamber for measuring the temperature of the plasma chamber. A water pump circulates water in tubes winded around the chamber to cool down the chamber. A chiller is used to cool the circulating water that reduces the temperature of chambers walls to room temperature.

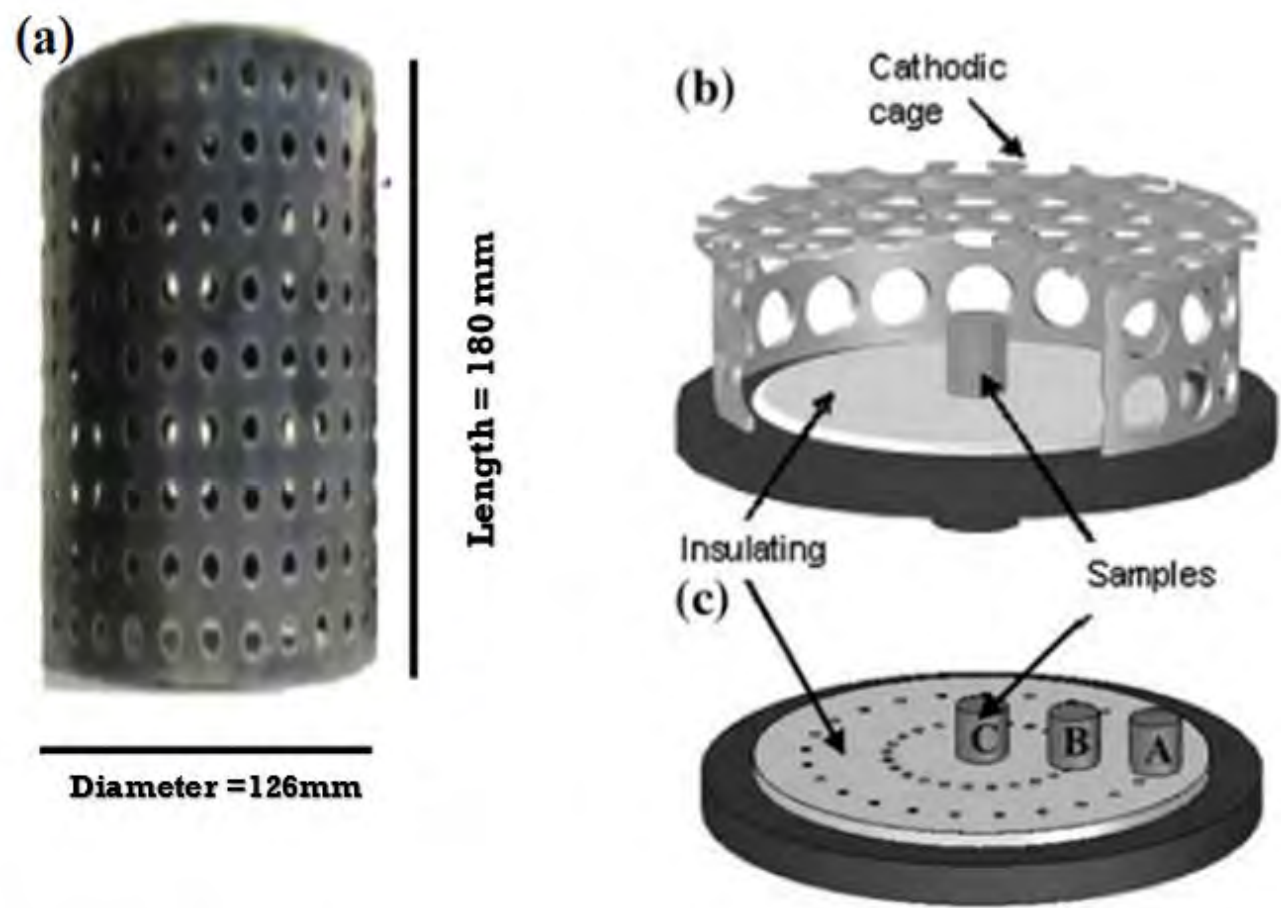

Figure 3.8: (a) Pictorial diagram of Cathodic cage. (b) Specimen placed inside cage (c) Specimens placed on the ceramic plate.

3.2.2 Cathodic cage

Cathodic cage used in experiment is made up of stainless steel, AISI 304. It is a hollow cylinder with open bottom has a height of 180 mm and diameter 126 mm. There are equally spaced small holes drilled at the side and top walls of the cage. Side and top holes have 8 mm and 6 mm

diameters respectively. The thickness of the cage walls is 3 mm. Specimens are placed inside the cage but 20 mm below the top wall. During experiment, the cage is given a negative potential and act as a cathode, that's why we name it cathodic cage or active screen. The specimens placed inside the cage at floating potential. The holes in the cage allow the plasma to pass through and reach the sample surface in a controlled and uniform manner. Cage technique gets rid over the arcing problem and temperature non-uniformity [64].

3.2.3 Vacuum System

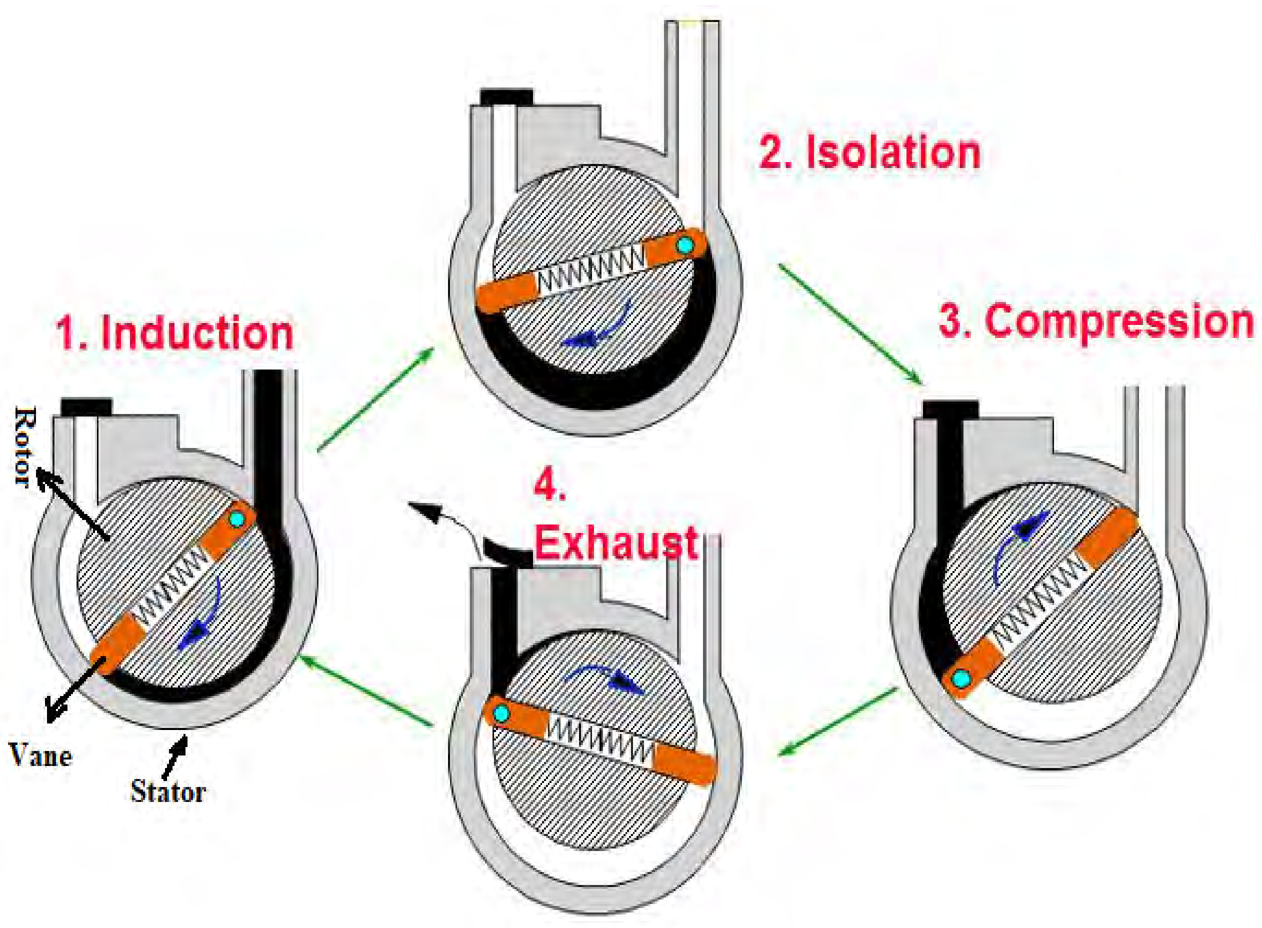

Figure 3.9: Working principle of rotary pump

It is necessary to evacuate the chamber to avoid oxidation and other impurities deposition during nitriding. A rotary van pump is used for the evacuation of CCPN chamber. This pump plays with volume and pressure of the gas and works on the principle of Boyle's law [61].

$$P_1V_1 = P_2V_2$$

Rotary pump makes use of rotational motion to reduce volume and increase pressure in such a way that the product of both quantities remains constant. It follows the four steps cyclic process as given in the following figure 3.9.

There are vanes connected through a spring passes through the rotor. Rotor rotates along with vanes between stator. Rotary pump lets the air inside in the first step (induction). The received air expands in the second step, inside a closed volume between the sweeping vanes. In the third step, air is compressed between rotating rod and outlet value. The compressed air finally exhausts through the value. The rotary pump used in the experiment can create a vacuum up to 10^{-3} mbar. A capsule gauge is used to measure the chamber pressure.

3.2.4 Power system

Pulse DC is used in the experiment. To convert AC of frequency $50\ Hz$ and voltage $250\ volts$, into high magnitude pulsed DC, a step-up transformer and a half wave rectifier are used. The transformer steps up the voltage $\sim 2kV$ and current $\sim 2A$. Rectifier, then allows only negative pulse to the cathode and anode is grounded. Pulse current of $1.2A$, duty cycle of 15% and frequency $40\ kHz$ are used in experiment. Ammeter circuit measures current and voltmeter measures voltage. All values are displayed on the screen of the power supply.

3.2.5 Gas Feeding

Gasses are used in the formation of plasma discharges. Argon, Nitrogen and hydrogen inlets are connected to the chamber for this purpose. The optimized mixture of these gasses is fed into the chamber with to produce glow discharge. Gas flow controller and mass flow measurement mechanism are also connected. $50\ sccm$ Argon is fed for $30\ minutes$ to sputter and clean the chamber maintaining a pressure of $1.5\ mbar$. After half an hour, $30\ sccm$ nitrogen and $20\ sccm$ hydrogen is injected into the chamber. This mixture has fed for 90 minutes. Flow meters measure the gas inlet values for each gas.

3.3 Characterization Techniques

3.3.1 X-rays Diffraction

X-rays Diffraction is a characterization procedure used to determine the structural properties of the material to be examined. It consists of x-ray source, target on which incoming x-

rays fall and an x-ray detector for detecting the outcoming x-rays from the target sample. It works on the principle of Bragg's law. It states that if an x-ray beam strike on the target sample and got reflected after hitting and interfere with each other to give an interference pattern. The results achieved from XRD is in the form of intensity peaks which determine the characteristics of the material. The relation of Bragg's law is specified by the famous equation [65].

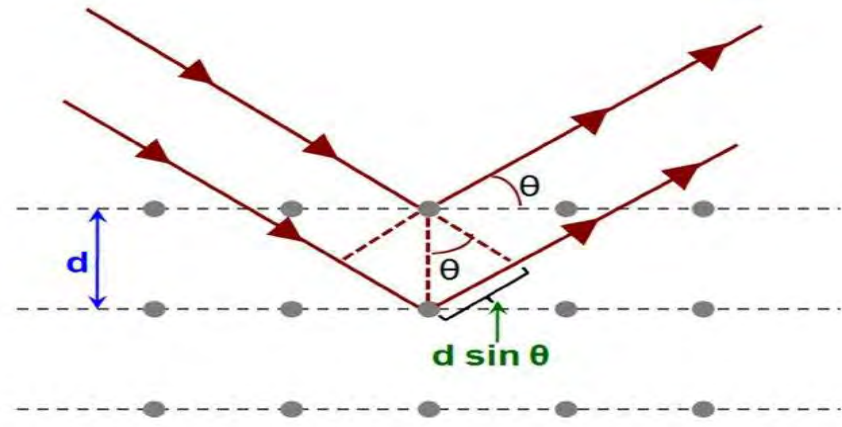

Figure 3.10: Interference pattern of Bragg's law

$$2d_{hkl}sin\theta = n\lambda$$

Where d_{hkl} is interplanar spacing between consecutive lattice planes, (hkl) is the Miller plane of the related peak, θ is the position of the peak on 2θ scale and λ is the wavelength of the x-ray used. Normally Copper kα radiations are used for x-ray diffraction. Furthermore, using Bragg's law lattice parameter and further crystallite size and lattice defects like dislocation and micro strain can be calculated.

$$\frac{1}{d_{hkl}^2} = \frac{h^2 + k^2 + l^2}{a^2}$$

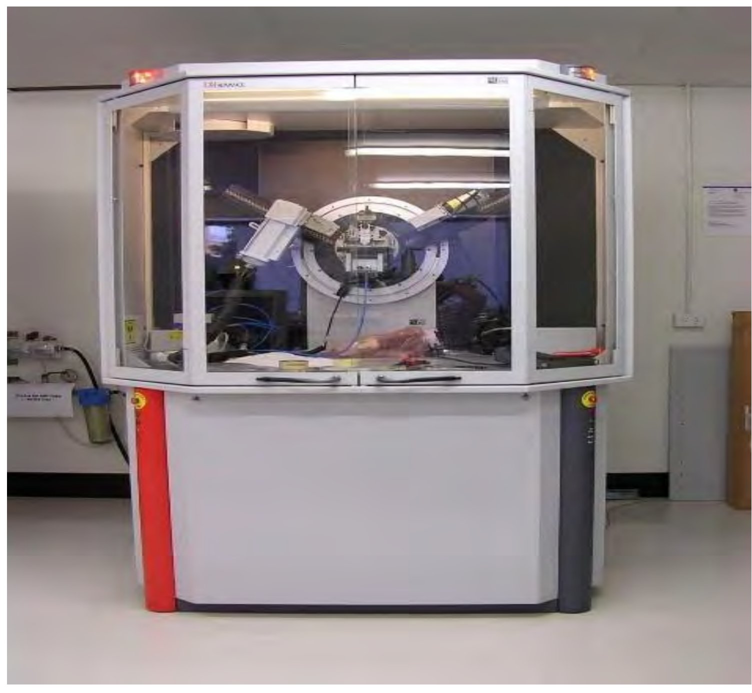

Figure 3.11: Pictorial diagram of X-Ray Diffraction Apparatus

3.3.2 Scanning Electron Microscope (SEM)

SEM is acronym for scanning electron microscope in which a concentrated beam of electrons is used for the generation of images of the specimen at very low dimensions. The beams electron interacts with the atoms of the sample and knock out the atomic electron from its shell. The vacancy of the removed electron is filled by the upper shell electron by emitting a photon in the high energy resolution called as x-rays. These x-rays contain information about the sample placed on the target. The rays are detected by special detectors and the final image of the sample is concluded. The image shows information about the surface features of an object that is how it looks, its textures. The morphology of the film like particle's size and shape, making up the object, the element and compound that the specimen is possessed of and relative amounts of elements and the arrangement of the atoms in the object. The advantage of electron microscope is that it magnifies the target at much lower levels from about 10 times up to 300,000 times and to high depth that is more than 30 times the depth of the ordinary light microscope [66].

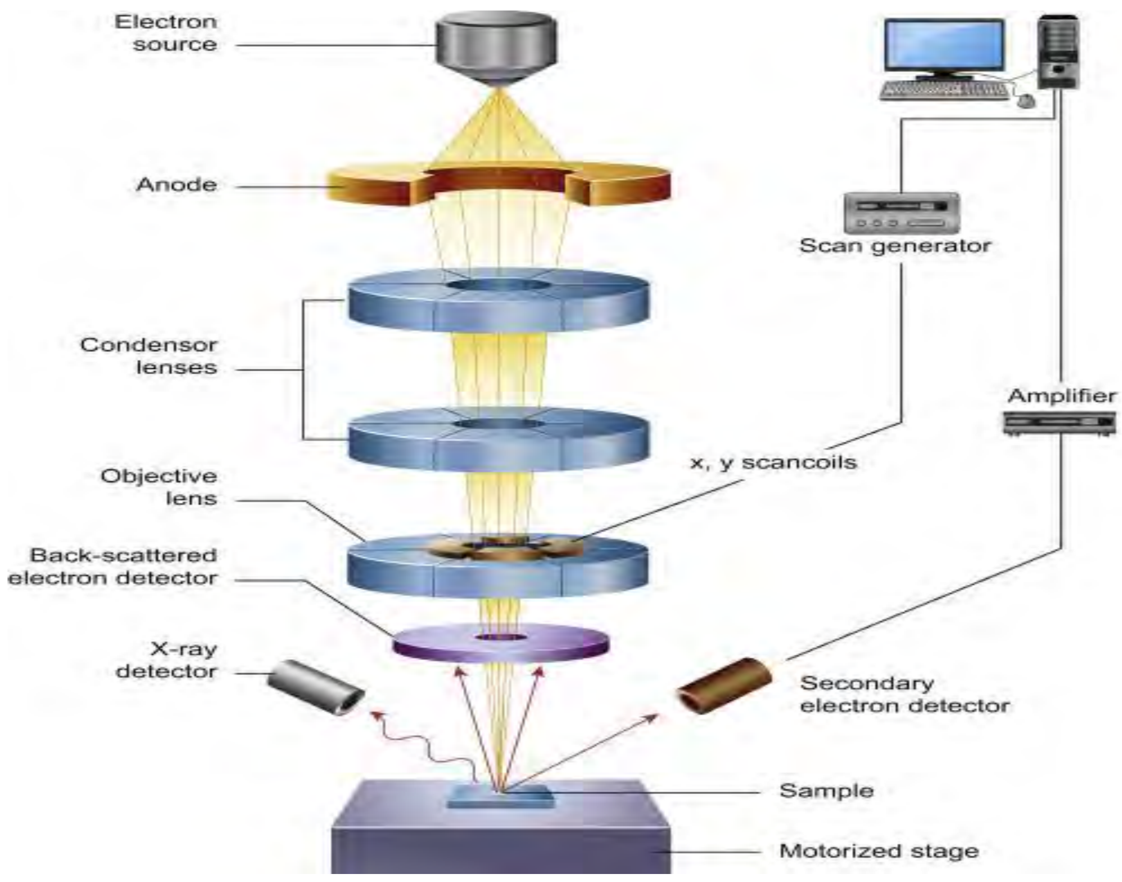

Figure 3.12: Diagram of Scanning electron Microscope (SEM)

3.3.3 Micro Hardness Test (MHT)

Hardness of the material is the measure of a material resistance to plastic deformation. There are different types of testers that are generally used which depend upon the nature of tests to be conducted. Specimen of metals are judged by Vickers hardness tester for measuring the hardness by forming an indent on the surface. It was developed by Smith and Sandland in 1921. The hardness of any material can be measured through by Vickers hardness tester.

3.3.3.1 Principle of Micro Hardness Test

Most commonly used hardness tester is Vickers hardness tester as shown in figure 3.13. As compared to other techniques, Vickers hardness test is multidimensional, as it can test the thin sections. The square type indentation in the test is easily and accurately measurable.

This test works on the principle of stress made by a known load. On the specimen surface, an indent is made by a known load and the area of indent is measured. Hardness is calculated through the following relation.

$$stress = \frac{load}{area\ of\ indent}$$

Figure 3.13: Pictorial diagram of Vickers hardness tester

Stress has the dimension of pressure. Indenter of particular dimensions is used, and its critical indentation dimensions are measured. Hardness is measured by indenters of low and high diagonal lengths which show high and low hardness values respectively. Indentation marks are becoming visible as the load increases. lower loads cause larger deviation in measurement which cause error. Therefore, maximum load should apply during the hardness test.

The micro hardness tester has a Diamond-pyramid with an angle of 136° [67]. Loads range between 10 gf and 500 gf are selected. The values of testing are expressed in terms of load and area of impression. Indenter impression on a sample is of square shape [68]. The diagonal lengths of square are seen and measured with the help of a microscope. Its magnification is adjusted with an ocular micrometer consists of moveable knife edges. These knife edges can be set at any position with the help of scale marked over there in millimeter.

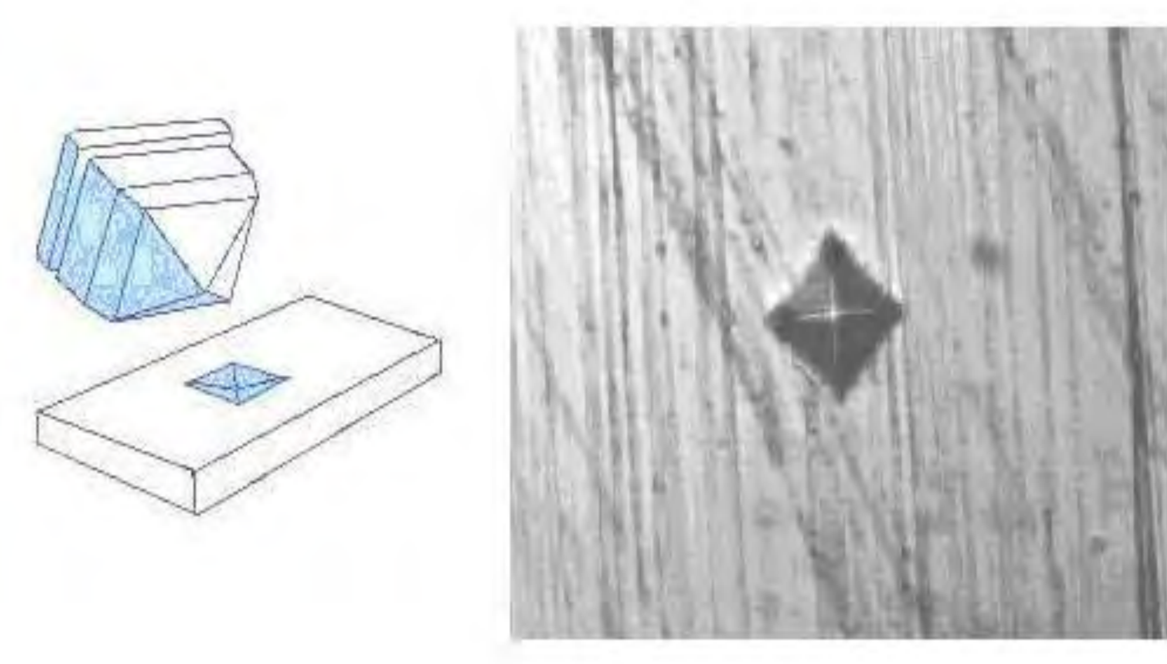

Figure 3.14: Indentation scheme of Vickers Hardness Tester

3.3.3.2 Micro Hardness Measurement

The specimen is carefully placed under a microscope, and a specific location for indentation is chosen. An indenter with a predetermined load is selected, ensuring suitability for the material being tested. The chosen indenter is used to create a distinct indentation on the specimen's surface as shown in figure 3.14. The microscope is employed to accurately identify and examine the created indentation. The diagonals of the indented area are measured as shown in figure 3.15. The process is systematically repeated using indenters with varying loads to obtain a comprehensive understanding of the material's properties.

The units HV tells the degree of hardness of a metal or material surface. to reduce the error and for more precession we take 5 reading at each load and then use their average. Hardness value is calculated by using the following formula

$$HV = \frac{2F \ \sin\frac{136^0}{2}}{d^2}$$

Where ‘HV’ shows the hardness value; ‘F’ is applied Load and “d” denotes the average value of two diagonals. The average value of diagonals is obtained by using the following formula.

$$d = \frac{d_1 + d_2}{2}$$

Where d_1 and d_2 are the diagonals of indent.

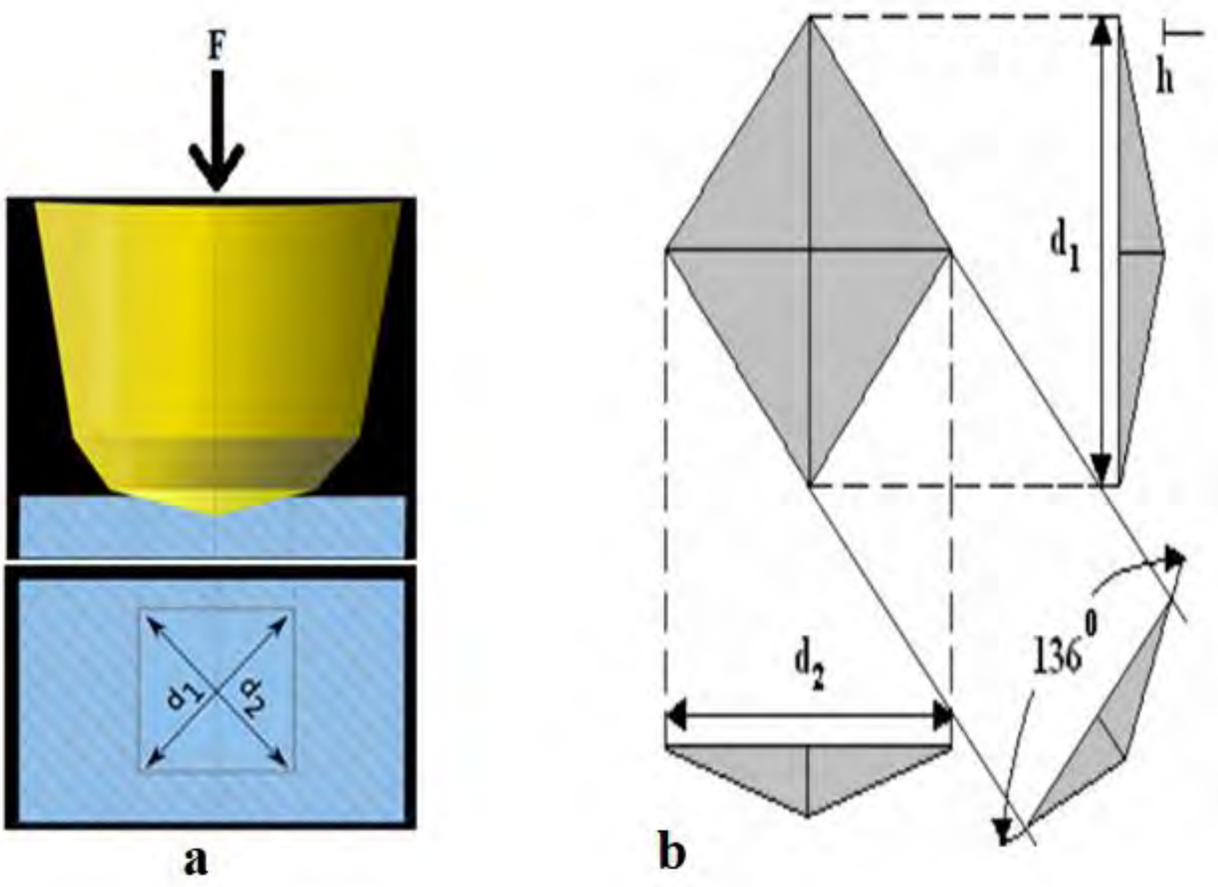

Figure 3.15: Schematic Indenter of hardness tester

Chapter No: 4

RESULTS AND DISCUSSION

Among inexpensive materials, high carbon steels are hard, wear resistive and relatively corrosion resistive. They are used for cutting tools and pressing metals. Therefore, high carbon steels are preferred, in making drill bits, knives, wood cutting tools and masonry nails. But high carbon steels are brittle and have poor weldability and malleability due to extra carbon content. They may cause fractures on employing stress. On the other hand, the medium carbon steels are less harder but are weldable and moldable. World demands a surface modification technique, to ensure and enjoy the hardness, wear resistance, malleability, corrosion resistance and weldability, all in a single material. Such materials have a high demand in aerospace, submarines and defense tools. The present work is an attempt to prepare a material like this.

Active screen plasma nitriding technique overcomes the flaws and disadvantages present in plasma nitriding, such as arcing and edge effects [69]. The uniform and thicker nitrided layer formed by this technique, is harder and wear resistive. The PVD (Physical Vapor Deposition) technique by magnetron sputtering has a number of advantages [27, 70]. It decreases the impurity level, easily controls the rate of film deposition and enables effective thin films [71]. The introduction of corrosion resistive element, even in the sea water, the Titanium Ti^{48}_{22} makes the work more interesting, fruitful and practically useful. The use of titanium in biomaterials is a proof of its inertness [72, 73]. In the present work, nitrided layer by ASPN (Active Screen Plasma Nitriding), followed by duplex Titanium layer by PVD (Physical Vapor Deposition), is formed over the substrate of High Carbon Steel, which obtains the top values of hardness, corrosion resistance and wear resistance along with unchanged intrinsic properties of the substrate.

4.1 Specimens Preparation

The $2mm$ thick sheet of High carbon steel is cut into square pieces of $10mm \times 10mm$ dimension. These pieces are polished with the help of METKON GRIPO ® 2V polisher. Silicon carbide papers of grades 220, 320, 600, 1000, 1500 and 2000 are used for polishing. Each specimen is then mirror polished by micro cloth using alumina powder. Then, specimens are placed in the acetone beaker and cleaned at $80\ C°$ with the help of ultrasonic cleaner for $25\ minutes$. After polishing and cleaning, the steel specimens are Nitrided with the help of ASPN (Active Screen Plasma Nitriding)

technique, under the optimized conditions. After nitriding, specimens are duplex treated with the help of PVD (Physical Vapor Deposition) technique.

The chemical composition with respect to weight percent of the high carbon steel used in the research work is given in the following table 6 [74].

Table 6: The chemical composition of Specimens.

S. No	Elements	Composition (wt %)
1	Carbon	1.23
2	Chromium	0.64
3	Manganese	0.34
4	Silicon	0.22
5	Nickle	0.07
6	Molybdenum	0.02
7	Phosphorus	0.006
8	Sulphur	0.006
9	Iron	97.467

4.2 Experimental parameters

Experimental parameters are the physical conditions under which the experiment is carried out. For each experimental setup in this experiment, physical parameters are given below.

4.2.1 ASPN (Active Screen Plasma Nitriding) Operation Parameters

The physical parameters of Active Screen Plasma Nitriding of specimens during experiment are given in the following table 7.

Table 7: Physical parameters of CCPN operation

S. No	*Physical Parameters*	*Numerical Value*
1	Base Pressure	10^{-3} mbar
2	Argon sputtering duration	30 Minuts
3	Argon sputtering flow rate	50 SCCM
4	Reactive sputtering Duration	1.5 Hours
5	Working Pressure	1.5 mbar
6	Hydrogen flow tare	20 SCCM
7	Nitrogen flow tare	30 SCCM
8	Temperature	400 ℃
9	Pulse Current	1.2 A
10	Frequency	40 kHz
11	Duty Cycle	15 %
12	Hight of the cylindrical cage	180 mm
13	Diameter of the cage	126 mm
14	Thickness of the cage walls	3 mm
15	Vertical separation between Specimens and cage (top)	20 mm

4.2.2 PVD (Physical Vapor Deposition) Operation Parameters.

The experimental parameters of Physical Vapor Deposition (PVD) operation of specimens, during the experiment are given in the following table 8.

Table 8: Physical Parameters of PVD operation

S. No	*Physical Parameters*	*Numerical Value*

1	Base Pressure	1.2×10^{-2} Pascals
2	Argon sputtering duration	30 Minutes
3	Argon sputtering flow rate	30 SCCM
4	Argon Pressure	7 Pascals
5	Magnetron Power	400 Watts
6	DC Voltage	-10 Volts
7	Ar/N Gas ratio	19/4 %
8	Reactive Sputtering duration	40 Minutes
9	Working Pressure	1.2×10^{-1} Pascals
10	Temperature	200 ℃

4.3 SEM observations

Scanning electron microscope is used for the surface morphology. Untreated, ASPN treated, single PVD treated and duplex treated specimens are characterized at a magnification of $\times$ 5,000.

4.3.1 Untreated Specimen

The surface of untreated is appeared scratched due to mechanical polishing [58, 59]. It has light grey, shiny and brighter appearance as shown in figure 4. 1(a). Bashir et al., 2017 and Raza et al., 2019 have reported the same SEM result for the untreated steel specimens.

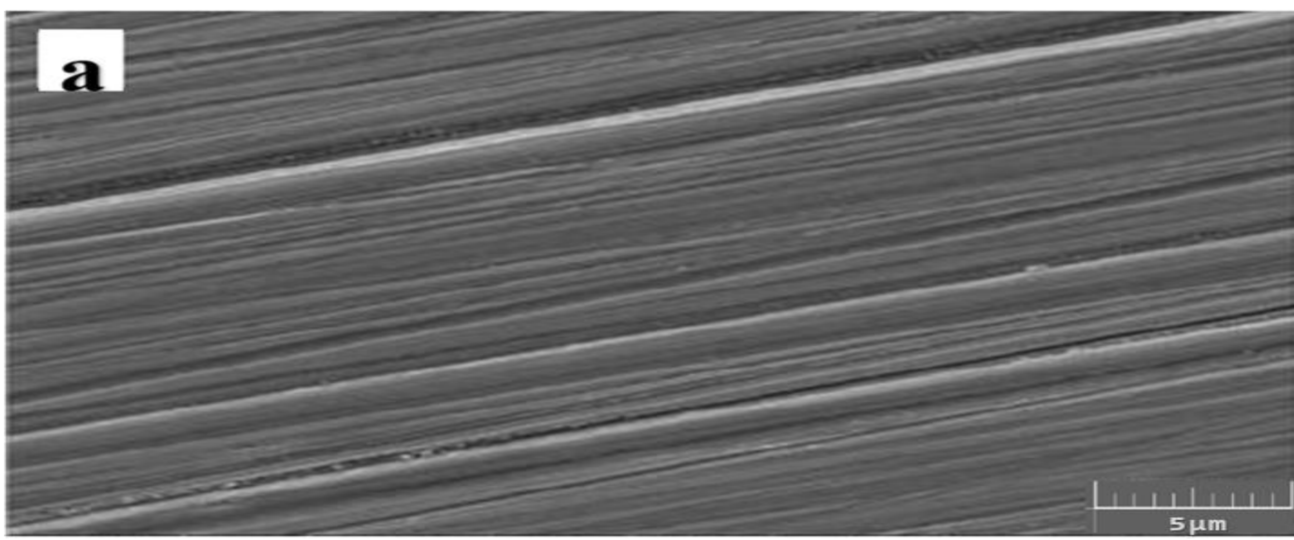

Figure 4.1(a): Micro-graph of untreated sciencemen has polishing scratches.

4.3.2 ASPN Treated Specimen

The ASPN treated specimen has white appearance under micrograph because of composite layer of nitride. The surface is smoother, because of uniform sputtering from the cathodic cage [58] as shown in figure 4.2(b). Surface smoothness is an indication of the enhancement of corrosion and wear resistance. Rough surfaces are always attacked by corrosion resistive materials and has a low wear resistance too. Specimens treated for longer time have porous surface, because bonds between carbon and nitrogen cannot bear high temperature for lengthy time duration [74].

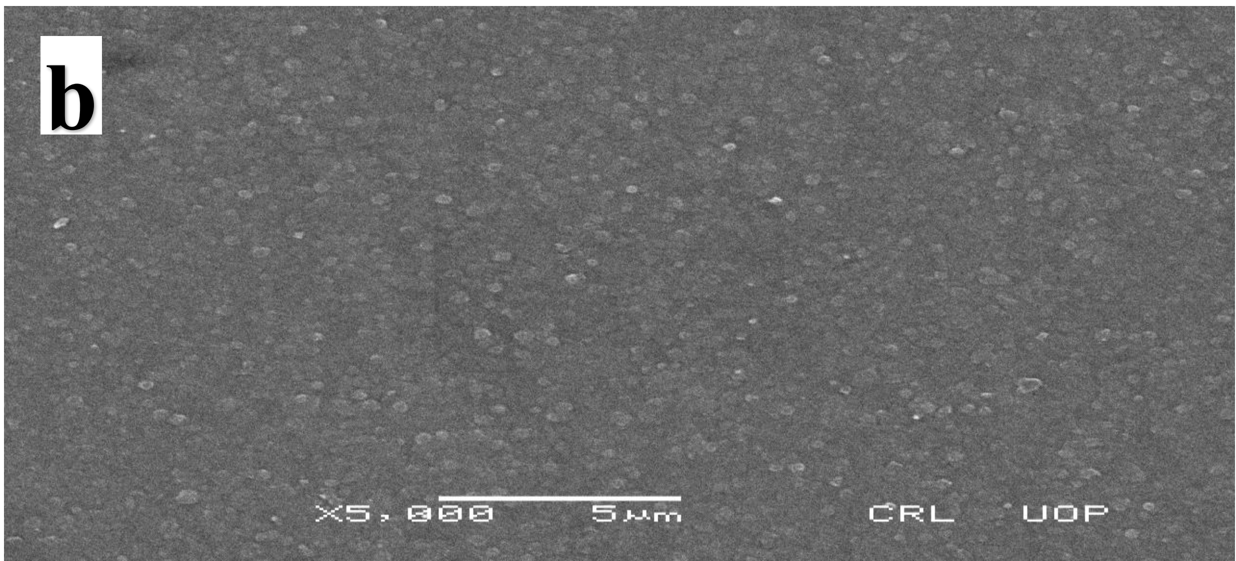

Figure 4.1(b): The SEM micrograph of ASPN treated specimen.

4.3.3 Single PVD Treated Specimen

In the present work, titanium-nitride layer is coated on the specimen by the treatment of PVD apparatus. But, it is the intrinsic flaw of PVD technique that titanium coated layer has voids and pinholes. The pinholes and voids defects are clearly visible in the micrograph shown in figure 4.3(c). pinholes are probably caused by the narrow polishing cavities which can not be completely covered. The oxygen (O_2) absorbed by the porous and granular surface contributes in making pinholes, when it escapes out. The voids are caused by thermal stresses during cooling under vacuum. Titanium nitride films has a porous columnar-microstructure, and there is always an opportunity for corrosive material to fix himself in that pores. To improve corrosion resistance, porosity must be removed [58, 59, 71, 75, 76].

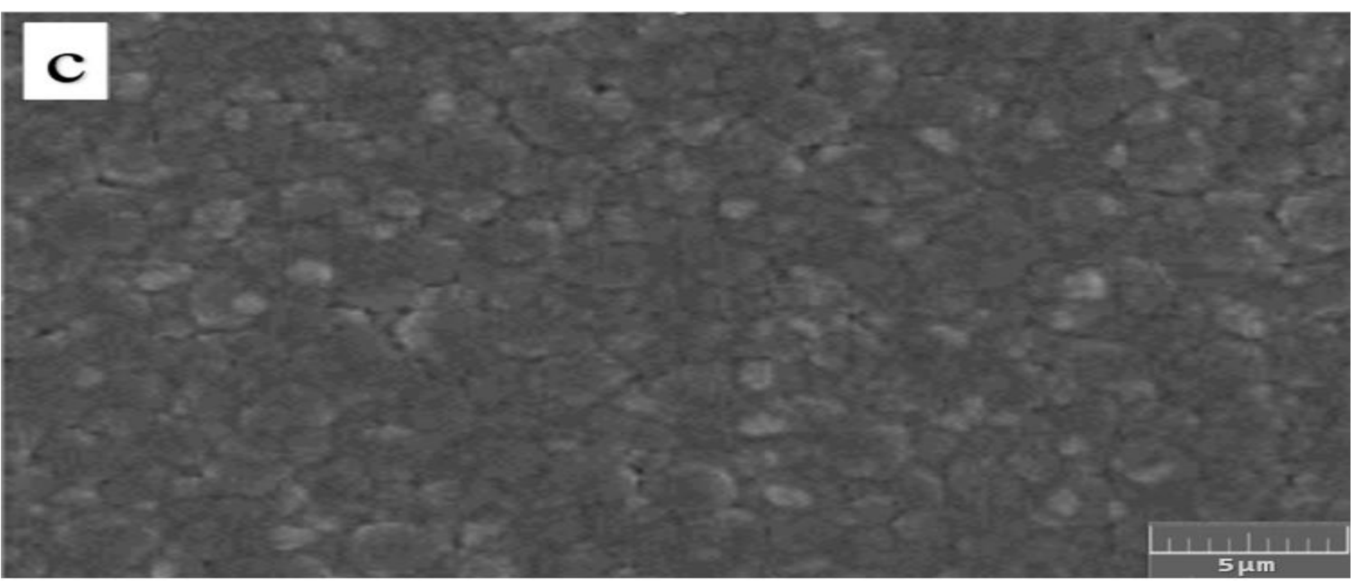

Figure 4.1(c): The SEM micrograph of single PVD treated specimen.

4.3.4 Duplex Treated Specimen

The ASPN treated sample are duplex treated by PVD. The surface of specimen is shown in the micrograph given the figure 4.4(d). The surface looks smoother as compered with the previous single coated specimen. The double coating technique works to get the surface smother and denser. There are no voids or pinhole defects, provided that the PVD parameters are kept the same, for both single and duplex treatments. The reason might be the diffusion of iron (Fe) from the steel substrate during the process of coating [77].

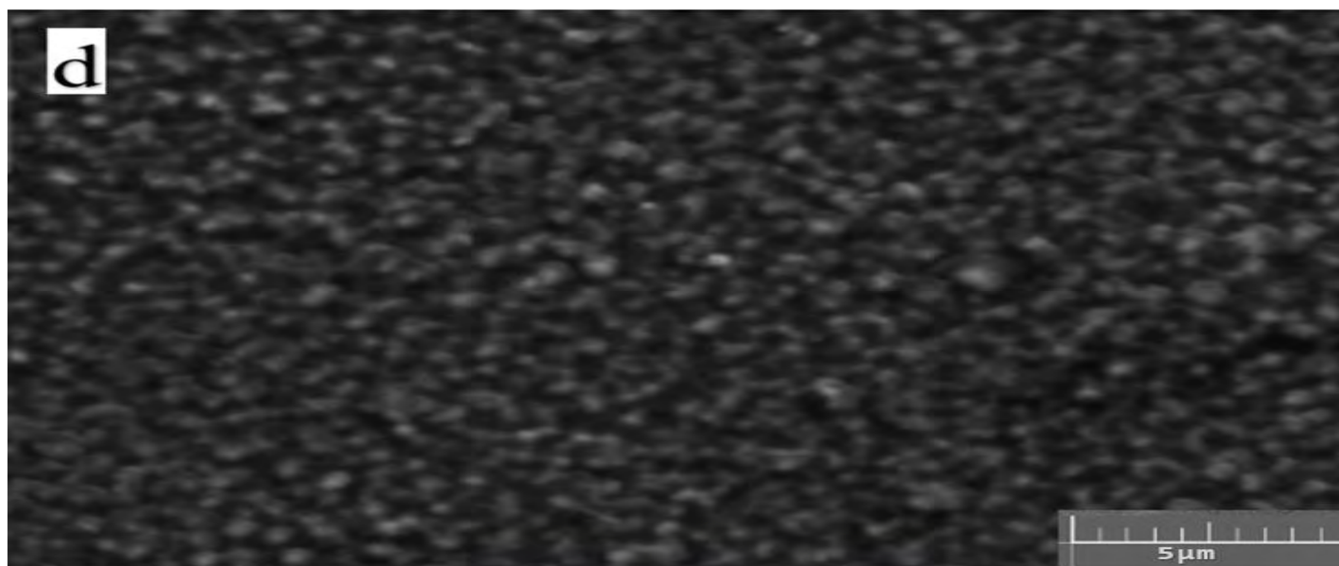

Figure 4.1(d): The SEM micrograph of Duplex PVD treated specimen

4.4 XRD Spectra

Crystallographic structure of the treated and untreated specimens are characterized by the X-ray diffractometer. The machine model is Philips (X Pert PRO MRD), uses Cu Kα of a wavelength, λ equals to $1.5418\ A°$. Diffractometer is operated at voltage of $40\ kV$ and current of $40\ mA$. The results obtained from the XRD are given. Here in figure 4.2, the intensity $\boldsymbol{I}$ in arbitrary units, is plotted against the grazing angle $\boldsymbol{2\theta}$ in the unit of degrees. The samples are characterized between $20°$ to $70°$ of the grazing angle. The scanning step length is kept 0.025 degrees per minutes.

4.4.1 XRD Spectrum of Untreated Specimen

The spectrum of untreated high carbon steel specimens, shows the iron and carbon intensity peaks. The iron peaks are dominant in intensity and the carbon have less dominant peaks. The peak at $44°$ is recorded the most intense peak in the untreated sample which corresponds to (101) plane of iron. Another iron peak found at an angle of 65°. Its (hkl) plane representation is (200). The carbon intensity peaks appeared at 32° and 39° angles. These peaks have lower intensities as shown in the figure 4.2. Angle 32° corresponds to (020) planes and 39° corresponds to (021) planes of carbon [74].

4.4.2 XRD Spectrum of ASPN Treated Specimen

During nitriding, the diffusion of nitrogen hides the iron and carbon peaks. Reaction of nitrogen with iron and carbon results iron and carbon nitrides. It is confirmed by the appearance of iron nitride and carbon nitride peaks such that nitride layer is deposited on the ASPN treated specimen. Treatment of the high carbon steel for a longer time results in the decrease of hardness [74]. It is observed that carbon nitride cannot stay against high temperature for a longer time. The same result had carried out by *Adnan saeed et al* in the treatment of high carbon steel under the title of "Pulsed dc Discharge in the Presence of Active Screen for Nitriding of High Carbon Steel". Carbon nitride C_3N_4 is the hardest material and its hardness is approachable to the diamond. It is later confirmed through Vickers micro hardness test that the ASPN treated sample is three times harder than the untreated high carbon steel as shown in table 9 and figure 4.3. The iron nitride is a corrosion resistive substance [78]. Both of these nitrides (iron nitride and carbon nitride) help in improving the tribological properties of the material.

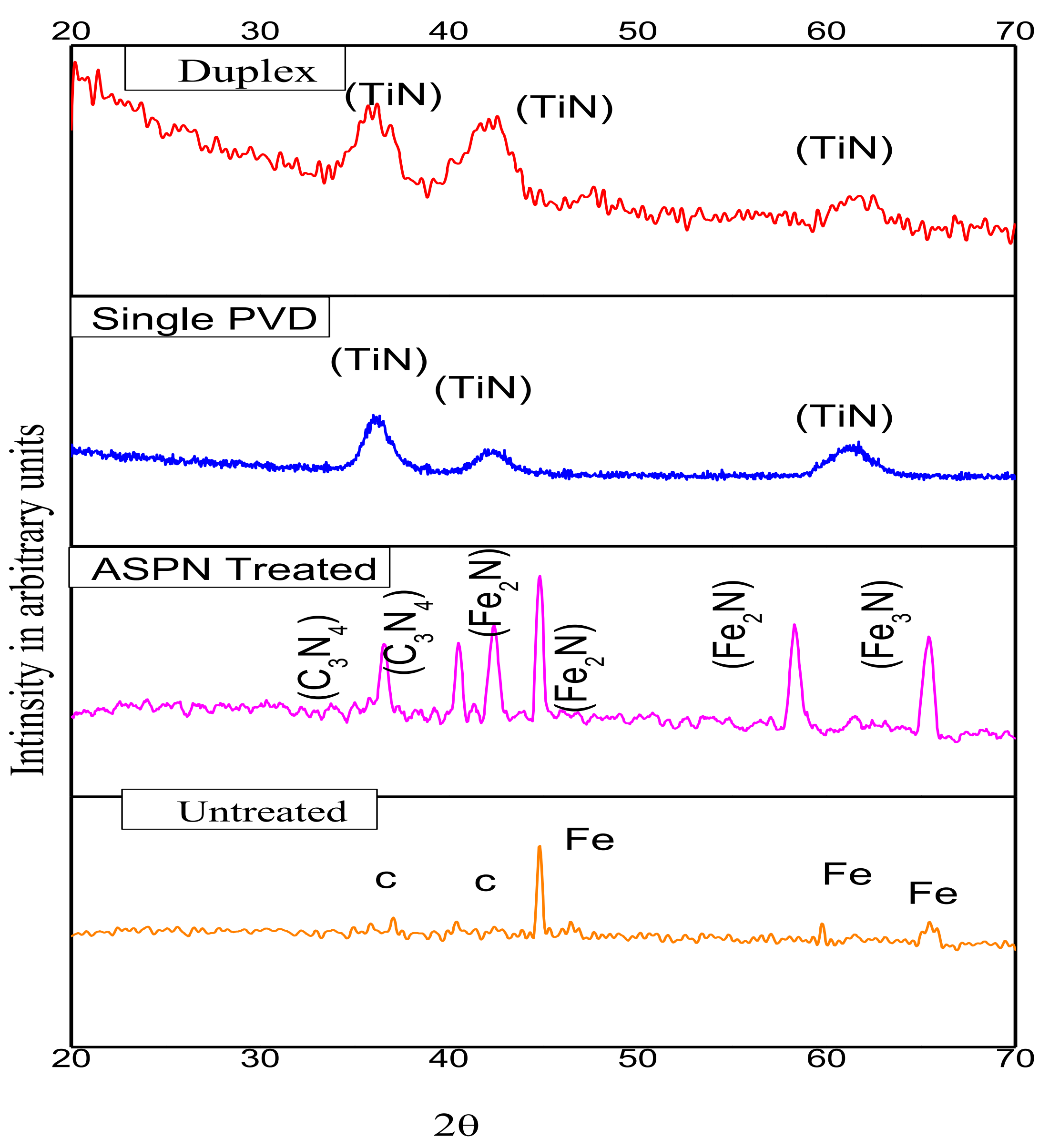

Figure 4.2: X-Ray diffraction analysis of the steel samples.

4.4.3 GIXRD Spectrum of Single PVD Treated Specimen

Figure 4.2 shows that titanium nitride peaks are observed at grazing angles of 36°, 42° and 61°. These angle corresponds (111), (200) and (220) planes. The maximum intensity is observed at 36° corresponds to (111) plane [58]. This plane indicates a special structure of TiN, namely the rock

salt or sodium chloride structure. The sodium chloride like structure is harder than hexagonal closed pack structure of TiN. It is because there are two slip planes in sodium chloride as compare with the three slip planes of hexagonal closed packed structure. Therefore it prevents sliding of planes, deformation, and brittleness. These factors plays a dominant role in the enhancement of hardness of the material.

4.4.4 GIXRD Spectrum of Duplex Treated Specimen

The Duplex treated sample contains three dominant peaks of Titanium Nitride as shown in figure 4.2. These peaks are observed at grazing angles of $36°, 42°$ and $61°$. The peak observed at 36° corresponds to (111) plane. The peak at $42°$ correspond to (200) and plane and the peak at $61°$ grazing angle corresponds to (220) plane. The more dominant peak is (111) like PVD treated specimen. Which indicates the sodium chloride structure of titanium nitride and provides hardness and avoids deformation and brittleness. It also has lower adatom mobility and contains larger number of atoms in a unit area at minimum energy positions. The other peak (200) becomes dominant which indicates an increase in the hardness of material. Which is later confirmed by the hardness test of the material.

4.5 Hardness observation

For the measurement of surface hardness, a micro hardness tester (Wilson 401 MVA Vickers) is used. This instrument is equipped with a 136^0 diamond indenter. The hardness of various specimens in the present experiment is measured as a function of applied loads. Figure 4.3 shows the hardness profile of plasma nitrided high carbon steel samples at a current of 1.2 A. Loads of range $10gf$ to $500\ gf$ are applied to obtain a micro-hardness profile. For precise reading, at least five readings are taken and then averaged, to find a single point on the graph shown in the figure 4.3. The readings are taken randomly for each load. For higher applied load such as $500\ gf$, a constant micro-hardness value of approximately 300 HV, representing the bulk hardness value is found. Graph shows a much enhanced micro hardness in the near surface region of all nitrided samples. The surface hardness increases continuously for smaller treatment times and up-to maximum of 932 HV, which is nearly a 3 times increase as compared to the high carbon steel bulk value. The surface hardness decreases for longer treatment time [74]. It is because the carbon nitrogen bonds formed on the surface cannot sustain the temperature for longer. The enhanced surface hardness can be indication to the nitrogen diffusion in to the high carbon steel sample by

nitrogen absorption. The high nitrogen quenching at the surface would provide a high nitrogen potential for diffusion. However, the low nitriding temperature used in this study (400^0 C) could justify a slow diffusion and a steep nitrogen gradient. Also the superficial hard nitriding layer containing nitrogen phase acts as a diffusion barrier for further nitrogen penetration. The macroscopic growth of the grain boundaries and the large internal stress showed the material hardness. The hardness of ASPN treated sample is the highest one which is slightly over three times the hardness of the base specimen. Duplex treated specimen is the next hard specimen of the experiment. It is slightly over two times the hardness of untreated specimen. It is probably because of thin layer deposited PVD technique. The hardness of single PVD specimen is slightly below two times the hardness of untreated specimen because of sole slim layer deposited over the specimen.

Table 9: Hardness profile of different specimens

Load (gf)	Untreated (HV)	ASPN (HV)	Single PVD (HV)	Duplex (HV)
10	302	922	553	680
25	293	898	540	624
50	290	605	486	558
100	286	555	386	436
200	281	405	329	402
300	260	322	313	310

500	235	242	234	239

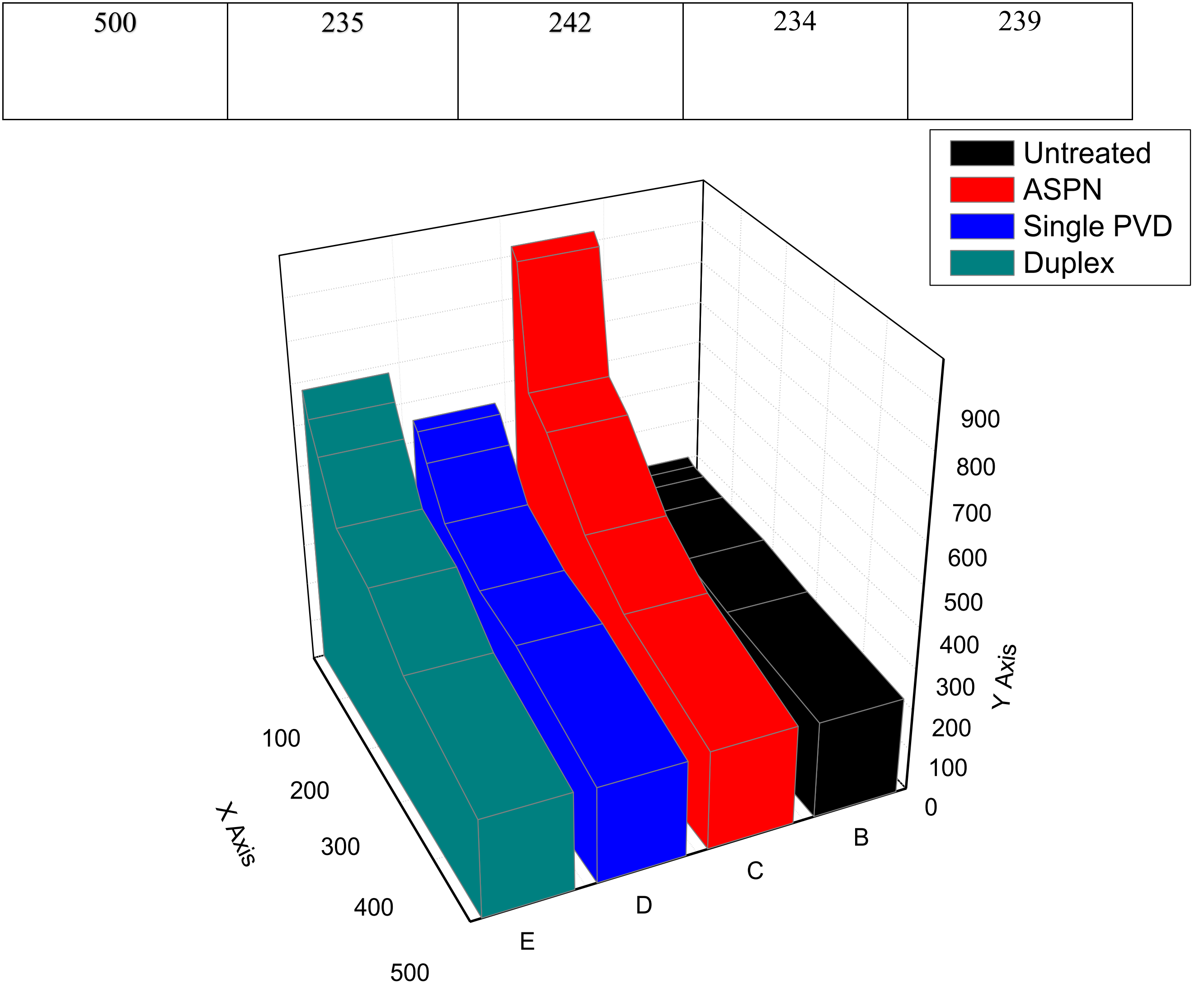

Figure 4.3: Hardness profile of the High carbon steel

4.5 Conclusion

The polished specimens of High Carbon Steel are treated through Active Screen Plasma Nitriding under optimized conditions of temperature (400 °C), pressure (1.5 mbar), power supply current (1.1A), gas flow of H_2 and N_2 (50 SCCM). The treatment time (1.5 Hrs) and gasses ratio($N_2/H_2 = 60/40$) are also kept optimized. Duplex layer is deposited on High Carbon Steel using ASPN and PVD techniques under optimized conditions. The specimens are then characterized by X-ray diffraction, SEM and micro hardness tester. The hardness of specimen treated only through ASPN has increased by 3 times due to the carbon nitride and iron nitride peaks observed in X-ray

diffraction. Other specimen of the same material is treated only by PVD technique and coated by a thin layer of titanium nitride. PVD treated specimen is slightly below the two times hardness of the untreated specimen, because of narrow slim coat of TiN. It is harder than base specimen because of the formation of sodium chloride structure of TiN. The main specimen of the present work is the Duplex PVD specimen which is treated by ASPN technique and later by PVD technique. The material coated on the surface of high carbon steel becomes more than two times harder compare with the untreated specimen. The TiN makes the material malleable, deformation resistive, inert and hard. The SEM micrographs are used to observe the surface morphology of the specimens. Nitriding layer diffused on the material is observed. The pinholes and voids in the PVD treated material has also seen. The post technique ASPN will be more efficient to enhance the tribological properties of the material and to overcome the problems of pores and pinholes. Post ASPN treatment can also increase the hardness of the material treated. Furthermore, alloy layer deposition on the specimen, will be more suitable for the amplification of the tribological properties of the high carbon steel.

4.6 Bibliography

[1] I. Azeem, J. Yue, L. Hoffmann, S. D. Miller, W. C. Straka III, and G. Crowley, "Multisensor profiling of a concentric gravity wave event propagating from the troposphere to the ionosphere," *Geophysical research letters,* vol. 42, pp. 7874-7880, 2015.

[2] A. Grill, *Cold Plasma Materials Fabrication: From Fundamentals to Applications*: Wiley, 1994.

[3] R. Fitzpatrick, *Plasma physics: an introduction*: Crc Press, 2014.

[4] R. J. Goldston and P. H. Rutherford, *Introduction to plasma physics*: CRC Press, 1995.

[5] F. F. Chen, "Introduction to Plasma Physics and Controlled Fusion," in *Introduction to Plasma Physics and Controlled Fusion*, ed: Springer, 2018, pp. E1-E1.

[6] F. F. Chen, *Introduction to plasma physics*: Springer Science & Business Media, 2012.

[7] Z. Xu and F. F. Xiong, *Plasma Surface Metallurgy: With Double Glow Discharge Technology—Xu-Tec Process*: Springer Singapore, 2017.

[8] M. Konuma, *Film Deposition by Plasma Techniques*: Springer Berlin Heidelberg, 2012.

[9] M. I. Boulos, P. Fauchais, and E. Pfender, *Thermal Plasmas: Fundamentals and Applications*: Springer US, 2013.

[10] P. Chabert and N. Braithwaite, *Physics of radio-frequency plasmas*: Cambridge University Press, 2011.

[11] A. Bogaerts, E. Neyts, R. Gijbels, and J. van der Mullen, "Gas discharge plasmas and their applications," *Spectrochimica Acta Part B: Atomic Spectroscopy,* vol. 57, pp. 609-658, 2002/04/05/ 2002.

[12] R. J. Shul and S. J. Pearton, *Handbook of Advanced Plasma Processing Techniques*: Springer Berlin Heidelberg, 2011.

[13] Y.-X. Liu, W. Jiang, X.-S. Li, W.-Q. Lu, and Y.-N. Wang, "An overview of diagnostic methods of low-pressure capacitively coupled plasmas," *Thin Solid Films,* vol. 521, pp. 141–145, 10/01 2012.

[14] Y. Sakamoto, S. Maeno, N. Tsubouchi, T. Kasuya, and M. Wada, "Comparison of Plasma Parameters in CCP and ICP Processes Appropriate for Carbon Nanotube Growth," *J. Plasma Fusion Res,* vol. 8, pp. 587-90, 2009.

[15] S. E. Hughes, *A Quick Guide to Welding and Weld Inspection*: Elsevier Science, 2009.

[16] D. K. NAYAK and R. Palai, "To study the effect of strain rate on tensile properties and high cycle fatigue behaviour of if steel," *Tech Project Report, National Institute of Technology, Rourkela,* 2013.

[17] H. Bhadeshia and R. Honeycombe, *Steels: microstructure and properties*: Butterworth-Heinemann, 2017.

[18] W. F. Smith, J. Hashemi, and S.-H. Wang, *Foundations of materials science and engineering* vol. 397: McGraw-hill New York, 2006.

[19] R. Singh, "Chapter 6 - Classification of Steels," in *Applied Welding Engineering (Second Edition)*, R. Singh, Ed., ed: Butterworth-Heinemann, 2016, pp. 57-64.

[20] R. Singh, "Chapter 5 - Stresses, Shrinkage, and Distortion in Weldments," in *Applied Welding Engineering (Second Edition)*, R. Singh, Ed., ed: Butterworth-Heinemann, 2016, pp. 201-238.

[21] W. Glaeser, *Materials for Tribology*: Elsevier Science, 1992.

[22] R. Singh, "Applied Welding Engineering."

[23] K. G. Budinski and M. K. Budinski, *Engineering Materials: Properties and Selection*: Pearson India Education, 2016.
[24] M. Blair, "Stainless Steels: Cast," in *Encyclopedia of Materials: Science and Technology*, K. H. J. Buschow, R. W. Cahn, M. C. Flemings, B. Ilschner, E. J. Kramer, S. Mahajan*, et al.*, Eds., ed Oxford: Elsevier, 2001, pp. 8798-8802.
[25] I. M. Association, I. M. A. Staff, T. Stainless, and T. S. Staff, *Practical Guidelines for the Fabrication of Duplex Stainless Steels*: BPR Publishers, 2009.
[26] Z. Xu and F. F. Xiong, "Plasma Nitriding," ed, 2017, pp. 13-21.
[27] D. M. Mattox, *Handbook of physical vapor deposition (PVD) processing*: William Andrew, 2010.
[28] M. Ohring, *Materials science of thin films*: Elsevier, 2001.
[29] S. Kasi, H. Kang, C. Sass, and J. Rabalais, "Inelastic processes in low-energy ion-surface collisions," *Surface Science Reports,* vol. 10, pp. 1-104, 1989.
[30] K. Wasa, I. Kanno, and H. Kotera, *Handbook of Sputter Deposition Technology: Fundamentals and Applications for Functional Thin Films, Nano-Materials and MEMS*: Elsevier Science, 2012.
[31] J. Millman, *Vacuum-tube and semiconductor electronics*: McGraw-Hill, 1958.
[32] C. Zhao, C. Li, H. Dong, and T. Bell, "Study on the active screen plasma nitriding and its nitriding mechanism," *Surface and Coatings Technology,* vol. 201, pp. 2320-2325, 2006.
[33] S. Ahangarani, A. Sabour, and F. Mahboubi, "Surface modification of 30CrNiMo8 low-alloy steel by active screen setup and conventional plasma nitriding methods," *Applied Surface Science,* vol. 254, pp. 1427-1435, 2007.
[34] C. Li and T. Bell, "Corrosion properties of active screen plasma nitrided 316 austenitic stainless steel," *Corrosion Science,* vol. 46, pp. 1527-1547, 2004.
[35] I. Soloshenko, V. Tsiolko, V. Khomich, A. Shchedrin, A. Ryabtsev, V. Y. Bazhenov*, et al.*, "Sterilization of medical productsin low-pressure glow discharges," *Plasma physics reports,* vol. 26, pp. 792-800, 2000.
[36] J.-S. Yoon, "Dielectric barrier discharge plasma actuator study for low Reynolds number flow control_Ph.D Thesis," 08/24 2015.
[37] J. R. Roth, *Industrial Plasma Engineering: Volume 1: Principles*: CRC Press, 1995.
[38] J. Russell and R. Cohn, *Paschen's Law*: Book on Demand, 2012.
[39] S. J. Anaghizi, P. Talebizadeh, H. Rahimzadeh, and H. Ghomi, "The Configuration Effects of Electrode on the Performance of Dielectric Barrier Discharge Reactor for NOxRemoval," *IEEE Transactions on Plasma Science,* vol. 43, pp. 1944-1953, 2015.
[40] F. Paschen, "On the potential difference required for spark initiation in air, hydrogen, and carbon dioxide at different pressures," *Annalen der Physik,* vol. 273, pp. 69-75, 1889.
[41] M. Endo and R. F. Walter, *Gas lasers*: CRC Press, 2016.
[42] A. Fridman and L. A. Kennedy, *Plasma Physics and Engineering*: Taylor & Francis, 2004.
[43] M. A. Lieberman and A. J. Lichtenberg, *Principles of Plasma Discharges and Materials Processing*: Wiley, 2005.
[44] S. L. Tong and W. W. Harrison, "Glow discharge mass spectrometric analysis of non-conducting materials," *Spectrochimica Acta Part B: Atomic Spectroscopy,* vol. 48, pp. 1237-1245, 1993/08/01/ 1993.
[45] J. Vlček, A. D. Pajdarová, and J. Musil, "Pulsed dc Magnetron Discharges and their Utilization in Plasma Surface Engineering," *Contributions to Plasma Physics,* vol. 44, pp. 426-436, 2004.

[46] H. Aghajani and S. Behrangi, "Pulsed DC Glow Discharge Plasma Nitriding," ed, 2017, pp. 71-125.
[47] Y. Lebedev, "Microwave discharges: Generation and diagnostics," *Journal of Physics: Conference Series,* vol. 257, p. 012016, 12/09 2010.
[48] S. Das, A. K. Mukhopadhyay, S. Datta, and D. Basu, "Prospects of microwave processing: An overview," *Bulletin of Materials Science,* vol. 32, pp. 1-13, 2009/02/01 2009.
[49] C. Prokisch, A. Bilgic, E. Voges, and J. A. C. Broekaert, *Analytical applications of microwave plasmas*, 1998.
[50] G. E. Totten and H. Liang, *Surface Modification and Mechanisms: Friction, Stress, and Reaction Engineering*: Taylor & Francis, 2004.
[51] E. J. Mittemeijer and M. A. J. Somers, *Thermochemical Surface Engineering of Steels: Improving Materials Performance*: Elsevier Science, 2018.
[52] H. Aghajani and S. Behrangi, *Plasma Nitriding of Steels*: Springer International Publishing, 2016.
[53] J. Dossett and G. Totten, "Fundamentals of Nitriding and Nitrocarburizing," 2013.
[54] K. M. Winter, J. Kalucki, and D. Koshel, "3 - Process technologies for thermochemical surface engineering," in *Thermochemical Surface Engineering of Steels*, E. J. Mittemeijer and M. A. J. Somers, Eds., ed Oxford: Woodhead Publishing, 2015, pp. 141-206.
[55] C. X. Li, T. Bell, and H. Dong, "A Study of Active Screen Plasma Nitriding," *Surface Engineering,* vol. 18, pp. 174-181, 2002/06/01 2002.
[56] C. X. Li, "Active screen plasma nitriding – an overview," *Surface Engineering,* vol. 26, pp. 135-141, 2010/02/01 2010.
[57] B. Edenhofer, "Physical and Metallurgical Aspects of Ionitriding. Pt. 1," *Heat Treatment Metals,* pp. 23-28, 1974.
[58] M. I. Bashir, M. Shafiq, M. Naeem, M. Zaka-ul-Islam, J. C. Díaz-Guillén, C. M. Lopez-Badillo*, et al.*, "Enhanced surface properties of aluminum by PVD-TiN coating combined with cathodic cage plasma nitriding," *Surface and Coatings Technology,* vol. 327, pp. 59-65, 2017.
[59] H. Raza, M. Shafiq, M. Naeem, M. Naz, J. Díaz-Guillén, and C. Lopez-Badillo, "Cathodic Cage Plasma Pre-treatment of TiN-Coated AISI-304 Stainless Steel for Enhancement of Mechanical Strength and Wear Resistance," *Journal of Materials Engineering and Performance,* vol. 28, pp. 20-32, 2019.
[60] A. K. Tareen, G. S. Priyanga, S. Behara, T. Thomas, and M. Yang, "Mixed ternary transition metal nitrides: A comprehensive review of synthesis, electronic structure, and properties of engineering relevance," *Progress in Solid State Chemistry,* vol. 53, pp. 1-26, 2019.
[61] C. A. Bishop, "4 - Pumping," in *Vacuum Deposition onto Webs, Films and Foils (Second Edition)*, C. A. Bishop, Ed., ed Oxford: William Andrew Publishing, 2011, pp. 63-80.
[62] P. Chiggiato, "Vacuum Technology for Ion Sources," *CAS-CERN Accelerator School: Ion Sources - Proceedings,* 04/03 2014.
[63] M. Naeem, J. Iqbal, F. Shabbir, M. Khan, J. Díaz-Guillén, C. Lopez-Badillo*, et al.*, "Effect of pulsed current on cathodic cage plasma nitriding of non-alloyed steel," *Materials Research Express,* vol. 6, p. 086537, 2019.
[64] H. Aghajani and S. Behrangi, "Active Screen Plasma Nitriding," in *Plasma Nitriding of Steels*, ed: Springer, 2017, pp. 127-159.
[65] S. Baskaran, "Structure and Regulation of Yeast Glycogen Synthase," 01/01 2010.

[66] B. J. Inkson, "2 - Scanning electron microscopy (SEM) and transmission electron microscopy (TEM) for materials characterization," in *Materials Characterization Using Nondestructive Evaluation (NDE) Methods*, G. Hübschen, I. Altpeter, R. Tschuncky, and H.-G. Herrmann, Eds., ed: Woodhead Publishing, 2016, pp. 17-43.
[67] D. Singh and R. Singla, *DOE: A Boom for Multi-Response Optimization of FSW: -A Guide for Effective Friction Stir Welding of Dissimilar Aluminium Alloys*, 2018.
[68] "Chapter 4 - Fundamentals of Materials Science," in *Craig's Restorative Dental Materials (Thirteenth Edition)*, R. L. Sakaguchi and J. M. Powers, Eds., ed Saint Louis: Mosby, 2012, pp. 33-81.
[69] M. C. Perju, M. Axinte, C. Nejneru, N. Cimpoesu, and C. A. Ţugui, "The active screen influence of edge effect in plasma nitriding," *IOP Conference Series: Materials Science and Engineering,* vol. 572, p. 012025, 2019/08/02 2019.
[70] O. Knotek, F. Löffler, and G. Krämer, "Process and advantage of multicomponent and multilayer PVD coatings," *Surface and Coatings Technology,* vol. 59, pp. 14-20, 1993/10/01/ 1993.
[71] K. Shukla, R. Rane, A. Joseph, P. Maity, and S. Mukherjee, "Structural, mechanical and corrosion resistance properties of Ti/TiN bilayers deposited by magnetron sputtering on AISI 316L," *Surface and Coatings Technology,* vol. 324, 05/01 2017.
[72] F. Findik, "Titanium Based Biomaterials," *Current Trends in Biomedical Engineering & Biosciences,* vol. 7, 08/23 2017.
[73] G. Manivasagam, A. K. Singh, A. Rajamanickam, and A. Gogia, "Ti based biomaterials, the ultimate choice for orthopaedic implants–A review," *Progress in Materials Science,* vol. 54, pp. 397-425, 05/01 2009.
[74] A. Saeed, A. Waheed Khan, F. Jan, M. Waqar, M. Abrar, Z. Ul - Islam Mujahid*, et al.*, "Pulsed dc Discharge in the Presence of Active Screen for Nitriding of High Carbon Steel," *Materials Research,* vol. 17, pp. 0-0, 07/01 2014.
[75] B. Subramanian and Muthurulandi, "Characterization of reactive magnetron sputtered nanocrystalline titanium nitride (TiN) thin films with brush plated Ni interlayer," *Journal of Applied Electrochemistry,* vol. 37, pp. 1069-1075, 09/01 2007.
[76] P. Panjan, M. Čekada, M. Panjan, and D. Kek-Merl, "Growth defects in PVD hard coatings," *Vacuum,* vol. 84, pp. 209-214, 2009/08/25/ 2009.
[77] G. I. Grigorov, K. G. Grigorov, M. Stojanova, J. L. Vignes, J. P. Langeron, P. Denjean*, et al.*, "Iron diffusion from pure Fe substrate into TiN buffer layers," *Physica C: Superconductivity,* vol. 241, pp. 397-400, 1995/01/15/ 1995.
[78] H. J. Spies, "6 - Corrosion behaviour of nitrided, nitrocarburised and carburised steels," in *Thermochemical Surface Engineering of Steels*, E. J. Mittemeijer and M. A. J. Somers, Eds., ed Oxford: Woodhead Publishing, 2015, pp. 267-309.

Turnitin Originality Report

Plasma Treated High Carbon Steel Under Optimized Conditions by Atta Ullah .

From DRSM (DRSML)

- Processed on 31-Jan-2020 09:20 PKT
- ID: 1249132993
- Word Count: 15226

Similarity Index
10%
Similarity by Source

Internet Sources:
2%
Publications:
4%
Student Papers:
9%

sources:

1 1% match (Internet from 01-May-2016)
http://www.materialsresearch.org.br/files/v17n4/v17n4a09.pdf

2 1% match (student papers from 13-Jul-2019)
Submitted to University of Science and Technology on 2019-07-13

3 1% match (student papers from 03-Oct-2014)
Submitted to Higher Education Commission Pakistan on 2014-10-03

4 < 1% match (student papers from 21-May-2014)
Submitted to Higher Education Commission Pakistan on 2014-05-21

5 < 1% match (publications)
K SREEHARSHA. "Cold Plasma Discharges", Principles of Vapor Deposition of Thin Films, 2005

6 < 1% match (student papers from 26-Feb-2019)
Submitted to Higher Education Commission Pakistan on 2019-02-26

7 < 1% match (student papers from 17-Feb-2010)
Submitted to Higher Education Commission Pakistan on 2010-02-17

8 < 1% match (Internet from 01-Nov-2014)
http://liu.diva-portal.org/smash/get/diva2:22370/FULLTEXT01

9 < 1% match (student papers from 03-Apr-2014)
Submitted to Higher Education Commission Pakistan on 2014-04-03

< 1% match (student papers from 27-Jul-2012)